87
1-21-83

I-7472

(1)

Dr. 1128

UCID- 19657-82

SUMMARY OF PHOTOCHEMICAL AND RADIATIVE DATA USED IN THE LLNL ONE-DIMENSIONAL TRANSPORT-KINETICS MODEL OF THE TROPOSPHERE AND STRATOSPHERE: 1982

Peters S. Connell and Donald J. Wuebbles

January 1983

Lawrence Livermore Laboratory

Work performed under the auspices of the U.S. Department of Energy by the Lawrence Livermore Laboratory under Contract W-7405-Eng-48.

UCID--19657-82

DE83 005490

SUMMARY OF PHOTOCHEMICAL AND RADIATIVE DATA USED IN THE LLNL ONE-DIMENSIONAL TRANSPORT-KINETICS MODEL OF THE TROPOSPHERE AND STRATOSPHERE: 1982*

Peters S. Connell and Donald J. Wuebbles
Lawrence Livermore National Laboratory
Livermore, CA 94550

INTRODUCTION

This report summarizes the contents and sources of the photochemical and radiative segment of the LLNL one-dimensional transport-kinetics model of the troposphere and stratosphere. Data include the solar flux incident at the top of the atmosphere, absorption spectra for O_2, O_3 and NO_2, and effective absorption coefficients for about 40 photolytic processes as functions of wavelength and, in a few cases, temperature and pressure. The current data set represents understanding of atmospheric photochemical processes as of late 1982 and relies largely on NASA Evaluation Number 5 of Chemical Kinetics and Photochemical Data for Use in Stratospheric Modeling, JPL Publication 82-57 (DeMore et al., 1982). Implementation in the model, including the treatment of multiple scattering and cloud cover, is discussed in Wuebbles (1981).

Wavelength dependent functions are expressed as averages over wavelength intervals. The range of wavelength considered, 133.3 to 735.0 nm, is divided into 148 contiguous non-overlapping bins. These are numbered from the long wavelength limit to allow extension of the model to the mesophere and arranged as shown in Table 1.

Table 1. Wavelength bin structure.

Bin #	Binwidth
1-8	10 nm bins centered from 660-730 nm,
9	7.5 nm bin from 647.5-655 nm,
10-77	5 nm bins centered from 310-645 nm,
78-128	500 cm^{-1} bins centered from 173.15-305.33 nm (32750-57750 cm^{-1})
129-142	1000 cm^{-1} bins centered from 139.84-170.94 nm (58500-71500 cm^{-1})
143-148	500 cm^{-1} bins centered from 133.75-138.40 nm (72250-74750 cm^{-1})

Incident Solar Flux

The incident solar flux used in the model is consistent with the recommendations of the WMO Global Ozone Research and Monitoring Project Report No. 11, The Stratosphere 1981 Theory and Measurements (1982). The tabulated values, SFLXIN(n), represent the solar irradiance at the top of the atmosphere integrated over wavelength bin, n,

$$SFLXIN(n) = \int_n I_{solar}(\lambda) d\lambda \ ,$$

in units of photons $cm^{-2}s^{-1}$. Values for bins 127-148 were taken from Ackerman (1970) and correspond to an integrated flux of 1.20 x 10^{12} photons cm^{-2} s^{-1} *over the range 133.3-175.4 nm, consistent with recent measurements* ranging from 0.52 to 1.5 x 10^{12} summarized in WMO (1982). The average of solar minimum and maximum measurements is used in the 175.4-200.0 nm region, where variability with solar activity is observed. Values from 200-735 nm follow directly from WMO (1982) and its sources. SFLXIN(n) is plotted in Figure 1 and tabulated in Appendix B.

Calculated Flux Between 0 and 55 km

Absorption by oxygen, ozone and nitrogen dioxide is considered in calculating solar fluxes appropriate to given altitudes and solar zenith angles, which are then corrected for scattering and cloud cover. The general expression for the local solar flux, SFLX(n,z,χ), in wavelength bin n at altitude z and solar zenith angle χ, is

$$\mathrm{SFLX}(n,z,\chi) = \mathrm{SFLXIN}(n)\exp[-\sec\chi\{\mathrm{COLO2}(z)\,\mathrm{SGO2}(n) + \mathrm{COLO3}(z)\,\mathrm{SGO3}(n) + \mathrm{COLNO2}(z)\,\mathrm{SGNO2}(n)\}],$$

where COLO2(z), COLO3(2), and COLNO2(z) are the vertical column abundances in molecules cm^{-2} above altitude z and SGO2(n), SGO3(n), and SGNO2(n) are the wavelength dependent absorption coefficients (shown in Figure 2), in units of cm^2 $molecule^{-1}$ (base e) for O_2, O_3, and NO_2, respectively. Column abundance for O_2, as well as temperature and pressure profiles, are those of the U. S. Standard Atmosphere (1976) unless temperature feedback is included. Overburdens of O_3 and NO_2 are evaluated within the model at each time step.

The Schumann-Runge bands of oxygen are covered by bins 110-126, 175.4-206.2 nm. In this region the product, sec χ COLO2(z) SGO2(n) is evaluated separately using the polynomial expressions developed by Allen and Frederick (1982) for O_2 transmittance as a function of wavelength, altitude and zenith angle. The coefficients for bins 110-114 were modified to account for the more recently established smaller contributions from the Herzberg continuum absorption. The expressions are presented in Appendix A. Transmittance calculations for these bins are extended above the model top at 56.25 km to 120 km. The numerical fits do not apply below 20 km, so sec χ SGO2(n) was fixed at its 20 km value for lower altitudes.

The O_2 Schumann-Runge continuum cross sections below 175.4 nm follow Ackerman (1970). The Herzberg continuum between 206.2 and 215 nm was assigned the average of the suggested values of Herman and Mentall (1982) and Frederick and Mentall (1982), based on stratospheric in situ uv measurements. Above 215 nm, cross sections were interpolated from the laboratory data of Shardanand and Rao (1977). The O_2 Herzberg continuum is presented graphically in Figure 3.

Ozone absorption coefficients were taken from the recommendations of Ackerman (1970), except in the region 232.6-347.5 nm, for which the recent results of Bass and Paur (1982) were used. They measured cross sections at temperatures of 228, 243 and 295 K and observed temperature dependence in a portion of the spectrum. Temperature dependent values are presented in Appendix A for wavelengths between 274 and 347.5 nm. In the model, absorption by ozone above the stratopause is characterized using their room temperature values, while below 55 km absorption coefficients are linearly interpolated between the data at the appropriate temperatures. For temperatures less than 228 K, the measured coefficient at 228 K is used.

Nitrogen dioxide absorption coefficients were interpolated from the recommendations of DeMore et al. (1982). The values at 235 K were used where they are given, otherwise the cross sections represent the room temperature spectrum.

Local Photodissociation Rate Constants

The photodissociation rate constants used in the rate equation for each photolytic process are calculated at each altitude by summing the product of the reactant absorption cross section, $\sigma(n)$, the quantum yield of the product channel, $\phi(n)$, and the appropriate solar flux, $SFLX(n,z,\chi)$, over wavelength bins,

$$j(z,\chi) = \sum_n \sigma(n)\phi(n)SFLX(n,z,\chi) .$$

The data for each process is compiled as the effective absorption cross section, $\sigma\phi$, for each bin in units of cm^2 $molecule^{-1}$ (base e) and presented in Appendix B. The individual processes are discussed below and summarized in Table 2, and the spectra are plotted in Figures 4-6.

1. $O_2 + h\nu \rightarrow 2\ O(^3P)$

The absorption spectrum has been discussed above. The quantum yield is 1.0 below the thermodynamic cutoff at 242 nm. Below 175 nm, the products are $O(^3P) + O(^1D)$, but this process is negligibly important in the stratosphere.

Table 2. Photodissociative processes presently included in the LLNL transport-kinetics model.

	Process	LLNL Code Identifier sq (i)
1.	$O_2 + h\nu \rightarrow 2O$	15
2.	$O_3 + h\nu \rightarrow O_2 + O(^1D)$	18
3.	$O_3 + h\nu \rightarrow O_2 + O$	16
4.	$H_2O + h\nu \rightarrow OH + H$	3
5.	$H_2O_2 + h\nu \rightarrow 2OH$	4
6.	$HOO + h\nu \rightarrow OH + O$	27
7.	$N_2O + h\nu \rightarrow N_2 + O(^1D)$	9
8.	$NO + h\nu \rightarrow N + O$	-
9.	$NO_2 + h\nu \rightarrow NO + O$	13
10.	$NO_3 + h\nu \rightarrow NO_2 + O$ (a)	14
	$\rightarrow NO + O_2$ (b)	36
11.	$N_2O_5 + h\nu \rightarrow NO_2 + NO_3$ (a)	10
	$\rightarrow 2NO_2 + O$ (b)	10
12.	$HONO + h\nu \rightarrow HO + NO$	11
13.	$HNO_3 + h\nu \rightarrow HO + NO_2$	7
14.	$HNO_4 + h\nu \rightarrow HO + NO_3$	28
15.	$HCl + h\nu \rightarrow H + Cl$	6
16.	$HOCl + h\nu \rightarrow OH + Cl$	29
17.	$ClO + h\nu \rightarrow Cl + O$	12+17
18.	$ClONO + h\nu \rightarrow Cl + NO_2$	22
19.	$ClONO_2 + h\nu \rightarrow Cl + NO_3$	24
20.	$CH_3Cl + h\nu \rightarrow CH_3 + Cl$	1
21.	$CH_3CCl_3 + h\nu \rightarrow$ Products (3Cl)	26
22.	$CCl_4 + h\nu \rightarrow$ Products (4Cl)	23
23.	$CFCl_3 + h\nu \rightarrow$ Products (3Cl)	19
24.	$CF_2Cl_2 + h\nu \rightarrow$ Products (2Cl)	20
25.	$CF_3Cl + h\nu \rightarrow$ Products (1Cl)	42
26.	$CHFCl_2 + h\nu \rightarrow$ Products (2Cl)	41
27.	$CHF_2Cl + h\nu \rightarrow$ Products (1Cl)	35
28.	$CFCl_2CFCl_2 + h\nu \rightarrow$ Products (4Cl)	43
29.	$CFCl_2CF_2Cl + h\nu \rightarrow$ Products (3Cl)	32
30.	$CF_2ClCF_2Cl + h\nu \rightarrow$ Products (2Cl)	33

Table 2. cont'd.

	Process	LLNL Code Identifier sq (i)
31.	$CF_3CF_2Cl + h\nu \rightarrow$ Products (1Cl)	34
32.	$CH_3CF_2Cl + h\nu \rightarrow$ Products (1Cl)	-
33.	$CH_2O + h\nu \rightarrow CHO + H$ (a)	30
	$\rightarrow H_2 + CO$ (b)	31
34.	$CH_3OOH + h\nu \rightarrow CH_3O + OH$	25
35.	$OCS + h\nu \rightarrow CO + S$	-
36.	$SO_2 + h\nu \rightarrow SO + O$	-
37.	$Cl_2 + h\nu \rightarrow 2Cl$	5
38.	$ClOO + h\nu \rightarrow ClO + O(^1D)$	8

2. $O_3 + h\nu \rightarrow O_2 + O(^1D)$

The absorption spectrum has been discussed above. The quantum yield expression recommended by DeMore et al. (1982) is used. This numerical fit to the observed wavelength and temperature dependence of the quantum yield approaches 0.9 below about 300 nm and 0.0 above 320 nm, as shown in Figure 7.

3. $O_3 + h\nu \rightarrow O_2 + O(^3P)$

The absorption spectrum has been discussed above. The quantum yield is the difference of 1.0 and the quantum yield of process 2, approaching 0.1 below 300 nm and 1.0 above 320 nm.

4. $H_2O + h\nu \rightarrow OH + H$

This process is of negligible importance in the stratosphere. Absorption coefficients are based on Thompson et al. (1963) and Watanabe and Zelikoff (1953). The indicated products represent the major pathway for this wavelength region (Okabe, 1978) and the quantum yield is assumed to be 1.0.

5. $H_2O_2 + h\nu \rightarrow 2\ OH$

The absorption coefficients were interpolated from DeMore et al. (1982) recommendations. The quantum yield is 1.0.

6. $HO_2 + h\nu \rightarrow 2OH + O$

The absorption coefficients were interpolated from DeMore et al. (1982) recommendations. The quantum yield is 1.0.

7. $N_2O + h\nu \rightarrow N_2 + O(^1D)$

The absorption coefficients were calculated from the numerical expression given by Selwyn et al. (1977), consistent with the recommendation of DeMore et al. (1982). Cross sections were calculated at a temperature of 225 K. The quantum yield was assumed to be 1.0.

8. $NO + h\nu \rightarrow N + O$

Effective absorption coefficients for NO are calculated using the polynomial expressions developed by Allen and Frederick (1982) from a numerical fit to photolysis constants calculated from experimental NO and O_2 line parameters (Frederick and Hudson, 1979). The derived coefficients depend on the local pressure and overhead oxygen column abundance, resulting from overlap of the predissociated NO δ bands with the O_2 Schumann-Runge bands. The expressions used are shown in Appendix A. Based on the bandwidths of the two vibrational components considered (Frederick and Hudson, 1979), the δ(0-0) band was split equally between bins 117 and 118, normalized to the correct integrated bandstrength, while the δ(1-0) band was divided 0.77:0.23 between bins 122 and 123.

9. $NO_2 + h\nu \rightarrow NO + O$

The absorption spectrum has been discussed above. The quantum yield is a function of wavelength and the recommended expression of DeMore et al. (1982) is used. The oxygen atom is released in the ^1D excited state at wavelengths less than about 240 nm, but this negligible contribution to atmospheric $O(^1D)$ is ignored in the model.

10. $NO_3 + h\nu \rightarrow NO_2 + O$ (a)
$\rightarrow NO + O_2$ (b)

The product $\sigma\phi$ for channels (a) and (b) has been tabulated at 1 nm intervals by Magnotta (1979). Some structure is lost in averaging over the 5 nm bins around 600 nm (Figure 8), but the wavelength integrated photolysis constants agree well with the recommendations of DeMore et al. (1982). (Note: The DeMore et al. recommendations are appropriate to photolysis constants above the atmosphere).

11. $N_2O_5 + h\nu \rightarrow NO_2 + NO_3$ (a)
$\rightarrow 2NO_2 + O$ (b)

The N_2O_5 absorption coefficients were taken from DeMore et al. (1982). A temperature of 240 K was used in calculating cross sections above 280 nm from the suggested expression. Quantum yields of 0.69 for process (a) and 0.31 for (b) were assigned, based on results reported by Connell et al. (1982).

12. $HONO + h\nu \rightarrow HO + NO$

The absorption coefficients were interpolated from the results of Stockwell and Calvert (1978), consistent with the recommendations of DeMore et al. (1982). The quantum yield is 1.0.

13. $HNO_3 + h\nu \rightarrow HO + NO_2$

The absorption cross sections were interpolated from the spectrum presented by DeMore et al. (1982). The quantum yield is 1.0.

14. $HNO_4 + h\nu \rightarrow HO + NO_3$

The absorption coefficients were taken from Molina and Molina (1980), which serves also as the NASA recommendation (DeMore et al., 1982). The quantum yield is assumed to be 1.0 and the products are taken to be $HO + NO_3$ by analogy to the observed products of $ClNO_3$ photolysis.

15. $HCl + h\nu \rightarrow H + Cl$

The absorption spectrum is taken from Inn (1975), also accepted as the NASA recommendation (DeMore et al., 1982). The quantum yield is 1.0.

16. $HOCl + h\nu \rightarrow HO + Cl$

The absorption spectrum is given in DeMore et al. (1982). The quantum yield is 1.0.

17. $ClO + h\nu \rightarrow Cl + O(^3P, ^1D)$

The absorption spectrum of ClO exhibits mostly continuum absorption below 263 nm, corresponding to $O(^1D)$ production, for which values from Watson (1977) were adopted (data of Johnston et al., 1969), assuming a quantum yield of 1.0. Above 270 nm, the spectrum is increasingly structured, showing a vibrational progression of the A-X transition. Since the rotational lines are broadened, predissociation is indicated between 310 and 270 nm and a quantum yield of 1.0 is assumed for the bands. Cross sections in this region are very roughly estimated from the results of Jourdain et al. (1978). Since the structure is finer than the bin spacing, it is averaged out.

18. $ClONO + h\nu \rightarrow Cl + NO_2$

The 231 K absorption coefficients of the Cl-O bonded isomer of $ClNO_2$ were used, based on DeMore et al. (1982) recommendations. The recommenced products are used and the quantum yield is 1.0.

19. $ClONO_2 + h\nu \rightarrow Cl + NO_3$

Absorption cross sections were interpolated from the 227 K results quoted by DeMore et al. (1982) for the wavelength region 190-400 nm. The quantum yield is 1.0 and there is strong experimental evidence for the choice of products (Margitan and Watson, manuscript in preparation, 1982).

20. $CH_3Cl + h\nu \rightarrow CH_3 + Cl$

The 255 K results of DeMore et al. (1982) were used for interpolation of the absorption coefficients. The quantum yield is 1.0.

21. $CH_3CCl + h\nu \rightarrow$ Products (3Cl)

The absorption coefficients are taken from the 230 K results of Vanlaethem-Meuree et al. (1979), which were presented for intervals consistent with the LLNL bin structure. This is also the NASA recommendation (DeMore et al., 1982). The photochemistry is simplified by assuming that all chlorine atoms are released *on absorption of a photon, while other products are ignored. This* assumption is made for the set of chlorocarbons (processes 21-31).

22. $CCl_4 + h\nu \rightarrow$ Products (4Cl)

The absorption coefficients were interpolated from data presented by DeMore et al. (1982). The quantum yield is 1.0.

23. $CFCl_3 + h\nu \rightarrow$ Products (3Cl)

The absorption coefficients were interpolated from data presented by DeMore et al. (1982). The quantum yield is 1.0.

24. $CF_2Cl_2 + h\nu \rightarrow$ Products (2Cl)

The absorption coefficients were interpolated from data presented by DeMore et al. (1982), corrected to 240 K using the expression given for temperature and wavelength dependence. The quantum yield is 1.0.

25. $CF_3Cl + h\nu \rightarrow$ Products (1Cl)

The absorption coefficients were interpolated from the geometric mean of the 208 K and 298 K data of Hubrich and Stuhl (1980). The quantum yield is 1.0.

26. $CHFCl_2$ + hν → Products (2Cl)

The absorption cross sections were interpolated from the 298 K data of Hubrich et al. (1977). The quantum yield is 1.0.

27. CHF_2Cl + hν → Products (1Cl)

The absorption cross sections were interpolated from the 298 K data of Hubrich et al. (1977). The quantum yield is 1.0.

28. $CFCl_2CFCl_2$ + hν → Products (4Cl)

No published data could be found for CFC-112, but its cross sections can be set to twice those of CFC-113 (process 29) with reasonable confidence, based on trends observed for the relationship of the number of chlorine atoms and CFC spectra.

29. $CFCl_2CF_2Cl$ + hν → Products (3Cl)

Absorption coefficients were taken from NASA Reference Publication 1049 (Hudson and Reed, 1979) for bins 102-120. Values in bins 98-101 were interpolated from the 298 K data of Hubrich and Stuhl (1980). The quantum yield is 1.0.

30. CF_2ClCF_2Cl + hν → Products (2Cl)

Absorption coefficients were taken from NASA 1049 (Hudson and Reed, 1979) for bins 106-120. Values in bins 103-105 were interpolated from the 298 K data of Hubrich and Stuhl (1980). The quantum yield is 1.0.

31. CF_3CF_2Cl + hν → Products (1Cl)

Absorption coefficients were taken from NASA 1049 (Hudson and Reed, 1979) for bins 113-120. Values in bins 109-112 were interpolated from the 298 K data of Hubrich and Stuhl (1980). The quantum yield is 1.0.

32. CH_3CF_2Cl + hν → Products (1Cl)

Absorption coefficients were interpolated from the 298 K data of Hubrich and Stuhl (1980). The quantum yield is 1.0.

33. CH_2O + hν → CHO + H (a)
→ H_2 + CO (b)

Absorption coefficients for channel (a), the radical products, were taken from the 223 K results of Bass et al. (1980). The quantum yields as a function of wavelength are an average of the results of Horowitz and Calvert (1978) and Moortgat and Warneck (1979). The product $\sigma\phi$ is closely similar to the recommendations of DeMore et al. (1982). Both curves are shown in Figure 9. The same sources were used for bins 74-92 for the molecular products channel (b). Between 330 and 360 nm, bins 67-73, the molecular products channel is predominant and the quantum yield exhibits wavelength and pressure dependence. Polynomial numerical expressions for these bins as a function of altitude were derived (Calvert, private communication, 1980) incorporating the various dependences, based on the results of Bass et al. (1980), Horowitz and Calvert (1978) and Moortgat and Warneck (1979). These results and the recommendations of DeMore et al. (1982) for channel (b) are shown in Figure 10. The expression and coefficients used in the fit are presented in Appendix A.

34. CH_3OOH + hν → CH_3O + OH

The absorption coefficients were interpolated from the results of Molina and Arguello (1979), also the basis of the NASA recommendation (DeMore et al., 1982). The quantum yield is assumed equal to 1.0 and the products are chosen to be analogous to H_2O_2 photolysis.

35. OCS + hν → CO + S

Absorption coefficients appropriate to the LLNL bin structure are tabulated by DeMore et al. (1982), at 225 K. The recommended quantum yield of 0.72 was also used.

36. $SO_2 + h\nu \rightarrow SO + O$

The absorption cross sections were derived from Figure 4 of Warneck et al. (1964), which shows the continuum absorption underlying the structured spectrum (Golomb et al., 1962) in the 170-230 nm region. The thermodynamic cutoff for SO_2 photolysis occurs at about 219 nm. Okabe (1978) has observed fluorescence from SO_2 excited states following excitation at wavelengths less than 220 nm. To avoid complications of the overlap of sharp structure with the Schumann-Runge bands of O_2, the bands were assumed to lead only to fluorescence, while the quantum yield for dissociation resulting from the continuum absorption was assumed equal to 1.0. This is undoubtedly an underestimate, since some photolysis should occur in the line spectrum from predissociation.

37. $Cl_2 + h\nu \rightarrow 2Cl$

Chlorine cross section values were interpolated from Watson (1977) and are consistent with NASA recommendations (DeMore et al., 1982). The quantum yield is 1.0.

38. $ClOO + h\nu \rightarrow ClO + O(^1D)$

Values for the absorption spectrum of the asymmetrical chlorine dioxide isomer were taken from Watson (1977). The quantum yield is 1.0.

REFERENCES

Ackerman, M., "Ultraviolet Solar Radiation Related to Mesospheric Processes," Aeronomica Acta, A, No. 77, 1980.

Allen, M., and J. E. Frederick, "Effective Photodissociation Cross Sections for Molecular Oxygen and Nitric Oxide in the Schumann-Runge Bands," J. Atmos. Sci., 39, 2066-2075, 1982.

Bass, A. M., L. C. Glasgow, C. Miller, J. P. Jesson, and D. L. Filkin, "Temperature Dependent Absorption Cross Sections for Formaldehyde (CH_2O): The Effect of Formaldehyde on Stratospheric Chlorine Chemistry," Planet. Space Sci., 28, 675-679, 1980.

Bass, A. M., and R. J. Paur, private communication, 1982.

Connell, P. S., F. Magnotta, D. Swanson, and H. S. Johnston, "Product Identification and Quantum Yield Determination in N_2O_5 Photolysis at Several Discrete Wavelengths Between 249 nm and 300 nm," presented at the 15th Informal Conference on Photochemistry, Stanford, CA, June 27-July 1, 1982.

DeMore, W. B., R. T. Watson, D. M. Golden, R. F. Hampson, M. Kurylo, C. J. Howard, M. J. Molina, and A. R. Ravishankara, "Chemical Kinetics and Photochemical Data for Use in Stratospheric Modeling, Evaluation Number 5," JPL Publication 82-57, Jet Propulsion Laboratory, California Institute of Technology, Pasadena, California, 1982.

Frederick, J. E., and R. D. Hudson, "Predissociation of Nitric Oxide in the Mesosphere and Stratosphere," J. Atmos. Sci., 36, 737-745, 1979.

Frederick, J. E., and J. E. Mentall, "Solar Irradiance in the Stratosphere: Implications for the Herzberg Continuum Absorption of O_2," Geophys. Res. Lett., 9, 461-464, 1982.

Golomb, D., K. Watanabe, and F. F. Marmo, "Absorption Coefficients of Sulfur Dioxide in the Vacuum Ultraviolet," J. Chem. Phys., 36, 958-960, 1962.

Herman, J. R., and J. E. Mentall, "O_2 Absorption Cross Sections (187-225 nm) from Stratospheric Solar Flux Measurements," J. Geophys. Res., 87, 8967-8975, 1982.

Horowitz, A., and J. G. Calvert, "Wavelength Dependence of the Quantum Efficiencies of the Primary Processes in Formaldehyde Photolysis at 25°C," Int. J. Chem. Kin., 10, 805-819, 1978.

Hubrich, C., and F. Stuhl, "The Ultraviolet Absorption of Some Halogenated Methanes and Ethanes of Atmospheric Interest," J. Photochem., 12, 93-107, 1980.

Hubrich, C., C. Zetzsch, and F. Stuhl, "Absorptionspektren von Halogenierten Methanen vcn 275 bis 160 nm bei Temperaturen von 298 und 208 K," Ber. Bunsenges. Phys. Chem., 81, 437-442, 1977.

Hudson, R. D., and E. I. Reed, "The Stratosphere: Present and Future," NASA Reference Publication 1049, 1979.

Inn, E. C. Y., "Absorption Coefficient of HCl in the Region 1400 to 2200A," J. Atmos. Sci., 32, 2375-2377, 1975.

Johnston, H. S., E. D. Morris, Jr., and J. Van den Bogaerde, "Molecular Modulation Kinetic Spectrometry. ClOO and ClO_2 Radicals in the Photolysis of Chlorine in Oxygen," J. Am. Chem. Soc., 91, 7712-7727, 1969.

Jourdain, J. L. G. LeBras, G. Poulet, J. Combourieu, P. Rigaud, and B. Leroy, "UV Absorption Spectrum of $ClO(A^2\pi-x^2\pi)$ up to the (1,0) Band," Chem. Phys. Lett., 57, 109-112, 1978.

Magnotta, F., "Absolute Photodissociation Quantum Yields of NO_3 and N_2O_5 by Tunable Laser Flash Photolysis-Resonance Fluorescence," Ph.D. Thesis, University of California, Berkeley and Lawrence Berkeley Laboratory, Materials and Molecular Research Division, LBL-9981, 1979.

Molina, M. J., and G. Arguello, "Ultraviolet Absorption Spectrum of Methylhydroperoxide Vapor," Geophys. Res. Lett., 6, 953-955, 1979.

Molina, L. T., and M. J. Molina, "Ultraviolet Absorption Cross Sections of HO_2NO_2 Vapor, "U. S. Dept. of Transportation Report FAA-EE-80-7, 1980.

Moortgat, G. K., and P. Warneck, "CO and H_2 Quantum Yields in the Photodecomposition of Formaldehyde in Air," J. Chem. Phys., 70, 3639-3651, 1979.

Okabe, H., Photochemistry of Small Molecules, John Wiley and Sons, Inc., New York, 1978.

Selwyn, G., J. Podolske, and H. S. Johnston, "Nitrous Oxide Ultraviolet Absorption Spectrum at Stratospheric Temperatures," Geophys. Res. Lett., 4, 427-430, 1977.

Shardan and A. D. Prasad Rao, "Collision-induced Absorption of O_2 in the Herzberg Continuum," J. Quant. Spectrosc. Radiat. Transfer, 17, 433-439, 1977.

Stockwell, W. R., and J. G. Calvert, "The Near Ultraviolet Absorption Spectrum of Gaseous HONO and N_2O_3," J. Photochem., 8, 193-203, 1978.

Thompson, B. A., P. Harteck, and R. R. Reeves, Jr., "Ultraviolet Absorption Coefficients of CO_2, CO, O_2, H_2O, N_2O, NH_3, NO, SO_2, and CH_4 Between 1850 and 4000A," J. Geophys. Res., 68, 6431-6436, 1963.

U. S. Standard Atmosphere, 1976, NOAA-S/T 76-1562, U. S. Government Printing Office, Washington, DC, 1976.

Vanlaethem-Meuree, H., J. Wisemberg, and P. C. Simon, "Ultraviolet Absorption Spectrum of Methylchloroform in the Vapor Phase," Geophys. Res. Lett., 6, 451-454, 1979.

Warneck, P., F. F. Marmo, and J. O. Sullivan, "Ultraviolet Absorption of SO_2: Dissociation Energies of SO_2 and SO," J. Chem. Phys., 40, 1132-1136, 1964.

Watanabe, K., and M. Zelikoff, "Absorption Coefficients of Water Vapor in the Vacuum Ultraviolet," J. Opt. Soc. Am., 43, 753-755, 1953.

Watson, R. T., "Rate Constants for Reactions of ClO_x of Atmospheric Interest," J. Phys. Chem. Ref. Data, 6, 871-917, 1977.

WMO Global Ozone Research and Monitoring Project Report No. 11, "The Stratosphere 1981 Theory and Measurements," World Meteorological Organization, Geneva, Switzerland, 1982.

Wuebbles, D. J., "A Summary of the LLNL One-Dimensional Transport-Kinetics Model of the Troposphere and Stratosphere: 1981," Lawrence Livermore National Laboratory, UCID-19185, 1981.

APPENDIX A: Numerical treatment of the O_2 Schumann-Runge bands, the temperature dependence of O_3 absorption, NO photolysis, and the temperature and pressure dependence of CH_2O photolysis.

O_2 Schumann-Runge Bands

The general expressions for the O_2 effective absorption cross sections for bin 110-126, taken from Allen and Frederick, are

$$\sigma_i(z,\chi) = \sigma_i(z,\chi=0°)(\sec\chi)^{-c_i(z)} ,$$

$$\log_{10}\sigma_i(z,\chi=0°) = \sum_{j=1,9} a_{ij}T(z)^{j-1}, \text{ for } i = 110 \text{ to } 112 ,$$

$$\log_{10}\sigma_i(z,\chi=0°) = \sum_{j=1,5} a_{ij}(\log_{10}P(z))^{j-1}, \ i = 113 \text{ to } 126 ,$$

$$\log_{10}c_i(z) = \sum_{j=1,5} b_{ij}(\log_{10}COLO2(z))^{j-1} ,$$

where,

$\sigma_i(z,\chi)$ = absorption cross section in bin i in units of cm^2 $molecule^{-1}$ (base e)

$P(z)$ = pressure in millibar

$T(z)$ = temperature in K

z = altitude

χ = solar zenith angle

COLO2(z) = vertical overhead column abundance of O_2 in molecules cm^{-2}.

The coefficients a_{ij} and b_{ij} are as tabulated in Allen and Frederick (1982), with the following changes in bins 110-114 to reflect the reduced Herzberg continuum absorption,

$a_{110,1} =$ -23.12205

$a_{111,1} =$ -23.13436

$a_{112,1} =$ -25.06084

$a_{112,2} =$ 0.03442774

$a_{112,3} =$ -2.212047×10^{-4}

$a_{112,4} =$ 6.186041×10^{-7}

$a_{112,5} =$ $-6.284394 \times 10^{-10}$

$a_{113,1} =$ -22.97610

$a_{114,1} =$ -22.75796

Temperature Dependence of the O_3 Spectrum

Ozone absorption cross sections in bins 70-85 are linearly interpolated with temperature between the 228, 243, and 295 K data of Bass and Paur (1982), averaged over the LLNL bin structure,

Bin	SGO3(228 K)	SGO3(243 K)	SGO3(295 K)
70	6.20(-22)*	7.60(-22)	1.030(-21)
71	8.64	8.30	1.63
72	2.21(-21)	2.26(-21)	3.51
73	5.16	5.38	7.54
74	1.022(-20)	1.059(-20)	1.41(-20)
75	2.19	2.28	2.82
76	4.49	4.65	5.54
77	9.00	9.34	1.064(-19)
78	1.76(-19)	1.78(-19)	2.00
79	3.34	3.32	3.61
80	5.94	6.08	6.39
81	1.050(-18)	1.069(-18)	1.120(-18)
82	1.74	1.76	1.82
83	2.70	2.73	3.09
84	3.91	3.95	4.02
85	5.33	5.36	5.41

*6.20(-22) = 6.20×10^{-22} cm^2 $molecule^{-1}$.

NO

The general expressions for NO photolysis,

$$\log_{10}\sigma_{NO}(i,z,\chi) = [\sum_{j=1,6} a_{ij}(\log_{10}P(z))^{j-1}] (\sec\chi)^{c_i(z)}$$

$$c_i(z) = \sum_{j=1,5} b_{ij}(\log_{10}COLO2(z))^{j-1}$$

where the meaning of the symbols is the same as for O_2 Schumann-Runge treatment, are taken from Allen and Frederick (1982), who also tabulate the associated coefficients a_{ij} and b_{ij}. The values calculated for the $\delta(0-0)$ and $\delta(1-0)$ bands are normalized as follows,

$$\sigma_{NO}(117) = 0.6\,\sigma_{NO}(\delta(0-0))$$

$$\sigma_{NO}(118) = 0.6\,\sigma_{NO}(\delta(0-0))$$

$$\sigma_{NO}(122) = 1.0\,\sigma_{NO}(\delta(1-0))$$

$$\sigma_{NO}(123) = 0.3\,\sigma_{NO}(\delta(1-0))$$

CH_2O

Absorption coefficients for the molecular products (H_2 + CO) channel of formaldehyde photolysis for bins 67-73, multiplied by the quantum efficiency, are calculated from the expression

$$10^{20}\sigma_i(z) = \sum_{j=1,5} a_{ij}z^{j-1} ,$$

where

$\sigma_i(z)$ = formaldehyde effective absorption coefficient in bin i at altitude z in cm^2 $molecule^{-1}$ (base e)

z = altitude in km .

The a_{ij} coefficients are tabulated on the next page.

a_{ij}	1	2	3	4	5
67	3.344(-4)	2.720(-4)	-4.974(-6)	2.818(-8)	0
68	7.549(-2)	2.032(-2)	-3.442(-4)	1.686(-6)	0
69	3.387(-2)	2.832(-3)	-2.804(-5)	-6.672(-8)	0
70	0.1673	-2.210(-4)	5.362(-4)	-1.708(-5)	1.501(-7)
71	0.6114	-2.851(-3)	1.371(-3)	-4.289(-5)	3.767(-7)
72	7.010(-2)	7.103(-4)	-6.392(-6)	-1.927(-8)	0
73	0.5748	3.485(-3)	-4.912(-5)	1.564(-7)	0

65H

APPENDIX B. LLNL wavelength bin structure, incoming solar flux and absorption cross sections.

bin	wlc	sflxin	sgo2	sgo3	sgno2	o3=o2+o(1d) [a]	o3=o2+o(3p) [a]	wlu	wll
1	730.00	4.9000e+15		5.1400e-22			5.1400e-22	7.3500e+02	7.2500e+02
2	720.00	4.9000e+15		6.4000e-22			6.4000e-22	7.2500e+02	7.1500e+02
3	710.00	5.0200e+15		7.9300e-22	5.2408e-21		7.9300e-22	7.1500e+02	7.0500e+02
4	700.00	5.1600e+15		9.1300e-22	6.6476e-21		9.1300e-22	7.0500e+02	6.9500e+02
5	690.00	5.0400e+15		1.1100e-21	8.0543e-21		1.1100e-21	6.9500e+02	6.8500e+02
6	680.00	5.2400e+15		1.3700e-21	8.9954e-21		1.3700e-21	6.8500e+02	6.7500e+02
7	670.00	5.2200e+15		1.7200e-21	1.1340e-20		1.7200e-21	6.7500e+02	6.6500e+02
8	660.00	5.1400e+15		2.0700e-21	1.1505e-20		2.0700e-21	6.6500e+02	6.5500e+02
9	651.25	3.8300e+15		2.4000e-21	1.6037e-20		2.4000e-21	6.5500e+02	6.4750e+02
10	645.00	2.6000e+15		2.6100e-21	1.8291e-20		2.6100e-21	6.4750e+02	6.4250e+02
11	640.00	2.6300e+15		2.7400e-21	2.0557e-20		2.7400e-21	6.4250e+02	6.3750e+02
12	635.00	2.6200e+15		3.1700e-21	1.9544e-20		3.1700e-21	6.3750e+02	6.3250e+02
13	630.00	2.6200e+15		3.4300e-21	2.3452e-20		3.4300e-21	6.3250e+02	6.2750e+02
14	625.00	2.6100e+15		3.6000e-21	2.7360e-20		3.6000e-21	6.2750e+02	6.2250e+02
15	620.00	2.6900e+15		3.9000e-21	3.1267e-20		3.9000e-21	6.2250e+02	6.1750e+02
16	615.00	2.5900e+15		4.2400e-21	3.5174e-20		4.2400e-21	6.1750e+02	6.1250e+02
17	610.00	2.6600e+15		4.5400e-21	3.5959e-20		4.5400e-21	6.1250e+02	6.0750e+02
18	605.00	2.6800e+15		4.8400e-21	4.1429e-20		4.8400e-21	6.0750e+02	6.0250e+02
19	600.00	2.6300e+15		4.8900e-21	4.6899e-20		4.8900e-21	6.0250e+02	5.9750e+02
20	595.00	2.6900e+15		4.6100e-21	5.2370e-20		4.6100e-21	5.9750e+02	5.9250e+02
21	590.00	2.6200e+15		4.4200e-21	5.7840e-20		4.4200e-21	5.9250e+02	5.8750e+02
22	585.00	2.7000e+15		4.3500e-21	5.5504e-20		4.3500e-21	5.8750e+02	5.8250e+02
23	580.00	2.6700e+15		4.5500e-21	6.4882e-20		4.5500e-21	5.8250e+02	5.7750e+02
24	575.00	2.6700e+15		4.7500e-21	7.4260e-20		4.7500e-21	5.7750e+02	5.7250e+02
25	570.00	2.5800e+15		4.6700e-21	8.3637e-20		4.6700e-21	5.7250e+02	5.6750e+02
26	565.00	2.5700e+15		4.3100e-21	9.3015e-20		4.3100e-21	5.6750e+02	5.6250e+02
27	560.00	2.5000e+15		3.8800e-21	9.1465e-20		3.8800e-21	5.6250e+02	5.5750e+02
28	555.00	2.5400e+15		3.3600e-21	1.0631e-19		3.3600e-21	5.5750e+02	5.5250e+02
29	550.00	2.5300e+15		3.1700e-21	1.2116e-19		3.1700e-21	5.5250e+02	5.4750e+02
30	545.00	2.5500e+15		3.0700e-21	1.3601e-19		3.0700e-21	5.4750e+02	5.4250e+02
31	540.00	2.4900e+15		2.8800e-21	1.5086e-19		2.8800e-21	5.4250e+02	5.3750e+02
32	535.00	2.5100e+15		2.7400e-21	1.6571e-19		2.7400e-21	5.3750e+02	5.3250e+02
33	530.00	2.5500e+15		2.5500e-21	1.8055e-19		2.5500e-21	5.3250e+02	5.2750e+02
34	525.00	2.4200e+15		2.0700e-21	1.9540e-19		2.0700e-21	5.2750e+02	5.2250e+02
35	520.00	2.3900e+15		1.7800e-21	2.1025e-19		1.7800e-21	5.2250e+02	5.1750e+02
36	515.00	2.3200e+15		1.6000e-21	2.2510e-19		1.6000e-21	5.1750e+02	5.1250e+02
37	510.00	2.4900e+15		1.5800e-21	2.2668e-19		1.5800e-21	5.1250e+02	5.0750e+02
38	505.00	2.4600e+15		1.6200e-21	2.4817e-19		1.6200e-21	5.0750e+02	5.0250e+02
39	500.00	2.4000e+15		1.2200e-21	2.6966e-19		1.2200e-21	5.0250e+02	4.9750e+02
40	495.00	2.4800e+15		9.0900e-22	2.8820e-19		9.0900e-22	4.9750e+02	4.9250e+02
41	490.00	2.3900e+15		8.2800e-22	3.1265e-19		8.2800e-22	4.9250e+02	4.8750e+02
42	485.00	2.3000e+15		8.4300e-22	3.3220e-19		8.4300e-22	4.8750e+02	4.8250e+02
43	480.00	2.5100e+15		7.1100e-22	3.5955e-19		7.1100e-22	4.8250e+02	4.7750e+02
44	475.00	2.4400e+15		4.8900e-22	3.9275e-19		4.8900e-22	4.7750e+02	4.7250e+02
45	470.00	2.3900e+15		4.0600e-22	4.1424e-19		4.0600e-22	4.7250e+02	4.6750e+02
46	465.00	2.3800e+15		3.6800e-22	4.2014e-19		3.6800e-22	4.6750e+02	4.6250e+02
47	460.00	2.3500e+15		3.5700e-22	4.5726e-19		3.5700e-22	4.6250e+02	4.5750e+02
48	455.00	2.3100e+15		2.1200e-22	5.1387e-19		2.1200e-22	4.5750e+02	4.5250e+02
49	450.00	2.3600e+15		1.7100e-22	5.3145e-19		1.7100e-22	4.5250e+02	4.4750e+02
50	445.00	2.1800e+15		1.4900e-22	5.4903e-19		1.4900e-22	4.4750e+02	4.4250e+02

bin	wlc	sflxin	sgo2	sgo3	sgno2	o3=o2+o(1d) a	o3=o2+o(3p) a	wlu	wll
51	440.00	2.0200e+15		1.2500e-22	5.6662e-19		1.2500e-22	4.4250e+02	4.3750e+02
52	435.00	1.9800e+15		8.6600e-23	5.8420e-19		8.6600e-23	4.3750e+02	4.3250e+02
53	430.00	1.6700e+15		6.8300e-23	6.0178e-19		6.8300e-23	4.3250e+02	4.2750e+02
54	425.00	1.8100e+15		6.5400e-23	6.2911e-19		6.5400e-23	4.2750e+02	4.2250e+02
55	420.00	1.9500e+15		3.9900e-23	6.3692e-19		3.9900e-23	4.2250e+02	4.1750e+02
56	415.00	1.9700e+15		3.1400e-23	6.4474e-19		3.1400e-23	4.1750e+02	4.1250e+02
57	410.00	1.8400e+15		2.9100e-23	6.5255e-19		2.9100e-23	4.1250e+02	4.0750e+02
58	405.00	1.7000e+15			6.6037e-19			4.0750e+02	4.0250e+02
59	400.00	1.6900e+15			6.6805e-19			4.0250e+02	3.9750e+02
60	395.00	5.3400e+14			6.0783e-19			3.9750e+02	3.9250e+02
61	390.00	1.1800e+15			6.5046e-19			3.9250e+02	3.8750e+02
62	385.00	8.9800e+14			6.4496e-19			3.8750e+02	3.8250e+02
63	380.00	1.1100e+15			6.5121e-19			3.8250e+02	3.7750e+02
64	375.00	9.7200e+14			5.7433e-19			3.7750e+02	3.7250e+02
65	370.00	1.0800e+15			5.7011e-19			3.7250e+02	3.6750e+02
66	365.00	1.0700e+15			5.8344e-19			3.6750e+02	3.6250e+02
67	360.00	8.2[illegible]0e+14		5.4900e-23	4.9629e-19		5.4900e-23	3.6250e+02	3.5750e+02
68	355.00	9.1400e+14		1.0900e-22	5.5199e-19		1.0900e-22	3.5750e+02	3.5250e+02
69	350.00	8.6900e+14		2.6600e-22	4.4966e-19		2.6600e-22	3.5250e+02	3.4750e+02
70	345.00	8.4400e+14		1.0300e-21	4.2930e-19		1.0300e-21	3.4750e+02	3.4250e+02
71	340.00	8.9400e+14		1.6300e-21	4.1748e-19		1.6300e-21	3.4250e+02	3.3750e+02
72	335.00	8.1500e+14		3.5100e-21	3.6066e-19		3.5100e-21	3.3750e+02	3.3250e+02
73	330.00	8.6100e+14		7.5400e-21	3.3750e-19		7.5400e-21	3.3250e+02	3.2750e+02
74	325.00	6.9600e+14		1.4120e-20	2.9415e-19		1.4120e-20	3.2750e+02	3.2250e+02
75	320.00	6.2200e+14		2.6200e-20	2.6108e-19		2.8200e-20	3.2250e+02	3.1750e+02
76	315.00	5.8300e+14		5.5400e-20	2.2420e-19	6.4200e-21	4.9000e-20	3.1750e+02	3.1250e+02
77	310.00	4.9500e+14		1.0640e-19	1.9638e-19	5.8600e-20	4.7800e-20	3.1250e+02	3.075[illegible]e+02
78	305.33	4.4000e+14		2.0000e-19	1.6600e-19	1.7400e-19	2.6200e-20	3.0770e+02	3.0300e+02
79	300.73	3.2400e+14		3.6100e-19	1.3156e-19	3.2490e-19	3.6100e-20	3.0300e+02	2.9850e+02
80	296.28	3.3900e+14		6.3900e-19	1.0697e-19	5.7510e-19	6.3900e-20	2.9850e+02	2.94[illegible]0e+02
81	292.00	3.4600e+14		1.1200e-18	1.0192e-19	1.0080e-18	1.1200e-19	2.9410e+02	2.8930e+02
82	287.78	2.1700e+14		1.6250e-18	7.7448e-20	1.6425e-18	1.8250e-19	2.8990e+02	2.85[illegible]0e+02
83	283.69	1.4800e+14		3.0900e-18	6.3718e-20	2.7810e-18	3.0900e-19	2.8[illegible]e+02	2.81[illegible]0e+02
84	279.74	7.5400e+13		4.0200e-18	5.5504e-20	3.6180e-18	4.0200e-19	2.8[illegible]e+02	2.7780e+02
85	275.89	1.0400e+14		5.4100e-18	4.1705e-20	4.8690e-18	5.4100e-19	2.7780e+02	2.7400e+02
86	272.14	1.0800e+14		6.8400e-18	3.2663e-20	6.1560e-18	6.8400e-19	2.7400e+02	2.7030e+02
87	268.50	1.1800e+14		8.1600e-13	2.7475e-20	7.3440e-18	8.1600e-19	2.7030e+02	2.6670e+02
88	264.94	1.0700e+14		9.5600e-18	2.4154e-20	8.6040e-18	9.5600e-19	2.6670e+02	2.6320e+02
89	261.44	4.4400e+13		1.0530e-17	1.8360e-20	9.4770e-18	1.0530e-18	2.6320e+02	2.5970e+02
90	258.04	4.6500e+13		1.1140e-17	1.6588e-20	1.0026e-17	1.1140e-18	2.5970e+02	2.5640e+02
91	254.79	2.2500e+13		1.1410e-17	1.5400e-20	1.0269e-17	1.1410e-18	2.5640e+02	2.5320e+02
92	251.59	1.8300e+13		1.1230e-17	1.6630e-20	1.0107e-17	1.1230e-18	2.5320e+02	2.5000e+02
93	248.44	1.8800e+13		1.0820e-17	1.1912e-20	9.7380e-18	1.0820e-18	2.5000e+02	2.4690e+02
94	245.39	1.8200e+13		1.0040e-17	3.4910e-20	9.0360e-18	1.0040e-18	2.4690e+02	2.4390e+02
95	242.44	2.0200e+13	8.9000e-25	9.1400e-18	6.7383e-20	8.2260e-18	9.1400e-19	2.4390e+02	2.4100e+02
96	239.54	1.3400e+13	1.4500e-24	8.0800e-18	9.5536e-20	7.2720e-18	8.0800e-19	2.4100e+02	2.3810e+02
97	236.69	1.5000e+13	2.0300e-24	6.9900e-18	1.6336e-19	6.2910e-18	6.9900e-19	2.3810e+02	2.3530e+02
98	233.94	1.3200e+13	2.5200e-24	5.9400e-18	1.6817e-19	5.3460e-18	5.9400e-19	2.3530e+02	2.3260e+02
99	231.24	1.5100e+13	2.9900e-24	4.8300e-18	3.1122e-19	4.3470e-18	4.8300e-19	2.3260e+02	2.2990e+02
100	228.59	1.3100e+13	3.3100e-24	4.0000e-18	3.0528e-19	3.6000e-18	4.0000e-19	2.2990e+02	2.2730e+02

						A	A		
bin	wlc	sflxin	sgo2	sgo3	sgno2	o3=o2+o(1d)	o3=o2+o(3p)	wlu	wll
101	226.00	1.3300e+13	3.5300e-24	3.2400e-18	3.0800e-19	2.9160e-18	3.2400e-19	2.2730e+02	2.2470e+02
102	223.44	1.5100e+13	3.9700e-24	2.5500e-18	3.4100e-19	2.2950e-18	2.5500e-19	2.2470e+02	2.2220e+02
103	221.00	1.1900e+13	4.3800e-24	1.9700e-18	3.8800e-19	1.7730e-18	1.9700e-19	2.2220e+02	2.1900e+02
104	218.59	1.0500e+13	4.8700e-24	1.5200e-18	4.0000e-19	1.3680e-18	1.5200e-19	2.1980e+02	2.1740e+02
105	216.19	8.4500e+12	5.4600e-24	1.1700e-18	4.0500e-19	1.0530e-18	1.1700e-19	2.1740e+02	2.1500e+02
106	213.89	7.7900e+12	5.9500e-24	8.5700e-19	4.0900e-19	7.7130e-19	8.5700e-20	2.1500e+02	2.1280e+02
107	211.64	7.2300e+12	6.3600e-24	6.2600e-19	3.9500e-19	5.6340e-19	6.2600e-20	2.1280e+02	2.1050e+02
108	209.39	4.2100e+12	6.7600e-24	4.8400e-19	3.8200e-19	4.3560e-19	4.8400e-20	2.1050e+02	2.0830e+02
109	207.24	2.5200e+12	7.1600e-24	4.1100e-19	3.8000e-19	3.6990e-19	4.1100e-20	2.0830e+02	2.0620e+02
110	205.15	2.0700e+12	7.4700e-24	3.5300e-19	3.6300e-19	3.1770e-19	3.5300e-20	2.0620e+02	2.0410e+02
111	203.05	1.6900e+12	7.8000e-24	3.2900e-19	3.1500e-19	2.9610e-19	3.2900e-20	2.0410e+02	2.0200e+02
112	201.00	1.4000e+12		3.2500e-19	2.7400e-19	2.9250e-19	3.2500e-20	2.0200e+02	2.0000e+02
113	199.00	1.1520e+12		3.3400e-19	2.3700e-19	3.0060e-19	3.3400e-20	2.0000e+02	1.9800e+02
114	197.05	1.0220e+12		3.7000e-19	2.2900e-19	3.3300e-19	3.7000e-20	1.9800e+02	1.9610e+02
115	195.15	9.0100e+11		4.0700e-19	2.3200e-19	3.6630e-19	4.0700e-20	1.9610e+02	1.9420e+02
116	193.25	6.5300e+11		4.3900e-19	2.4500e-19	3.9510e-19	4.3900e-20	1.9420e+02	1.9230e+02
117	191.40	6.3300e+11		4.7800e-19	2.8000e-19	4.3020e-19	4.7800e-20	1.9230e+02	1.9050e+02
118	189.60	5.4600e+11		5.2600e-19	2.9500e-19	4.7340e-19	5.2600e-20	1.9050e+02	1.8870e+02
119	187.80	4.9500e+11		5.8500e-19		5.2650e-19	5.8500e-20	1.8870e+02	1.8690e+02
120	186.05	3.7200e+11		6.3800e-19		5.7420e-19	6.3800e-20	1.8690e+02	1.8520e+02
121	184.35	3.1400e+11		6.8800e-19		6.1920e-19	6.8800e-20	1.8520e+02	1.8330e+02
122	182.65	3.3200e+11		7.2900e-19		6.5610e-19	7.2900e-20	1.8350e+02	1.8180e+02
123	181.00	2.8700e+11		7.6300e-19		6.8670e-19	7.6300e-20	1.8180e+02	1.8020e+02
124	179.40	2.3400e+11		7.8600e-19		7.0740e-19	7.8600e-20	1.8020e+02	1.7860e+02
125	177.80	2.1600e+11		8.0100e-19		7.2090e-19	8.0100e-20	1.7860e+02	1.7700e+02
126	176.20	1.7200e+11		8.0900e-19		7.2810e-19	8.0900e-20	1.7700e+02	1.7540e+02
127	174.65	1.8300e+11	2.7400e-19	8.4000e-19		7.5600e-19	8.4000e-20	1.7540e+02	1.7390e+02
128	173.15	1.4400e+11	4.5800e-19	8.5700e-19		7.7130e-19	8.5700e-20	1.7390e+02	1.7240e+02
129	170.94	2.3200e+11	7.2200e-19	8.1700e-19		7.3530e-19	8.1700e-20	1.7240e+02	1.6950e+02
130	168.09	1.7600e+11	1.2300e-18	8.1400e-19		7.3260e-19	8.1400e-20	1.6960e+02	1.6670e+02
131	165.29	1.1900e-11	2.0800e-18	8.6600e-19		7.7940e-19	8.6600e-20	1.6670e+02	1.6390e+02
132	162.59	5.4900e+10	3.4500e-18	9.7700e-19		8.7930e-19	9.7700e-20	1.6390e+02	1.6130e+02
133	160.00	6.4000e+10	4.9700e-18	1.2000e-18		1.0800e-18	1.2000e-19	1.6130e+02	1.5870e+02
134	157.44	4.7500e+10	6.5800e-18	1.6300e-18		1.4670e-18	1.6300e-19	1.5870e+02	1.5620e+02
135	155.00	3.6000e+10	8.2400e-18	2.1900e-18		1.9710e-18	2.1900e-19	1.5620e+02	1.5380e+02
136	152.64	2.9000e+10	9.9100e-18	2.9300e-18		2.6370e-18	2.9300e-19	1.5380e+02	1.5150e+02
137	150.34	2.6600e+10	1.1500e-17	3.6900e-18		3.3210e-18	3.6900e-19	1.5150e+02	1.4920e+02
138	148.09	2.3300e+10	1.2900e-17	4.4700e-18		4.0230e-18	4.4700e-19	1.4920e+02	1.4700e+02
139	145.94	1.8200e+10	1.4100e-17	5.2300e-18		4.7070e-18	5.2300e-19	1.4700e+02	1.4490e+02
140	143.84	1.3000e+10	1.4800e-17	5.6600e-18		5.0940e-18	5.6600e-19	1.4490e+02	1.4280e+02
141	141.79	1.0100e+10	1.4000e-17	6.2800e-18		5.6520e-18	6.2800e-19	1.4280e+02	1.4080e+02
142	139.84	7.6000e+09	1.3600e-17	7.1700e-18		6.4530e-18	7.1700e-19	1.4080e+02	1.3890e+02
143	138.40	3.1000e+09	1.3200e-17	7.9700e-18		7.1730e-18	7.9700e-19	1.3890e+02	1.3790e+02
144	137.45	2.7400e+09	1.2300e-17	1.0500e-17		9.4500e-18	1.0500e-18	1.3790e+02	1.3700e+02
145	136.50	2.5700e+09	9.5000e-18	1.3500e-17		1.2150e-17	1.3500e-18	1.3700e+02	1.3600e+02
146	135.55	3.0900e+09	7.2300e-18	1.5400e-17		1.3860e-17	1.5400e-18	1.3600e+02	1.3510e+02
147	134.65	1.9900e+09	4.5500e-18	1.6500e-17		1.4850e-17	1.6500e-18	1.3510e+02	1.3420e+02
148	133.75	1.2400e+10	2.3000e-18	1.5100e-17		1.3590e-17	1.5100e-18	1.3420e+02	1.3330e+02

bin	wlc	h2o	h2o2	hoo	n2o	no2	no3=no2+o	no3=no+o2	n2o5
12	635.00						2.3000e-20		
13	630.00						4.3800e-19	3.5000e-20	
14	625.00						1.7900e-18	3.3000e-19	
15	620.00						1.1100e-18	2.7000e-19	
16	615.00						9.6600e-19	3.7000e-19	
17	610.00						8.8800e-19	4.5000e-19	
18	605.00						2.4600e-18	1.2700e-18	
19	600.00						2.3100e-18	1.1300e-18	
20	595.00						3.8600e-18	1.8300e-18	
21	590.00						5.7100e-18	2.5000e-18	
22	585.00						3.9500e-18	3.5000e-19	
23	580.00						4.3200e-18		
24	575.00						3.7300e-18		
25	570.00						3.3300e-18		
26	565.00						3.2000e-18		
27	560.00						3.7700e-18		
28	555.00						3.2100e-18		
29	550.00						2.7600e-18		
30	545.00						2.0900e-18		
31	540.00						2.0800e-18		
32	535.00						2.3000e-18		
33	530.00						2.1500e-18		
34	525.00						1.6400e-18		
35	520.00						1.5900e-18		
36	515.00						1.5400e-18		
37	510.00						1.4500e-18		
38	505.00						1.2100e-18		
39	500.00						1.0900e-18		
40	495.00						1.0700e-18		
41	490.00						9.7600e-19		
42	485.00						7.6200e-19		
43	480.00						7.2000e-19		
44	475.00						6.7800e-19		
45	470.00						5.7300e-19		
46	465.00								
47	460.00								
48	455.00								
49	450.00								
50	445.00								
51	440.00								
52	435.00								
53	430.00								
54	425.00								
55	420.00					6.0000e-21			
56	415.00					2.3000e-20			
57	410.00					5.2000e-20			
58	405.00					2.1000e-19			
59	400.00					4.0000e-19			
60	395.00					4.3000e-19			

bin	wlc	h2o	h2o2	hno	n2o	no2	no3=no2+o	no3=no+o2	n2o5
61	390.00					4.2000e-19			
62	385.00					4.0000e-19			
63	380.00					4.0000e-19			9.2700e-23
64	375.00					4.3000e-19			1.3200e-22
65	370.00					4.9000e-19			1.8900e-22
66	365.00					4.9000e-19			2.7000e-22
67	360.00					4.0000e-19			3.8600e-22
68	355.00					4.1000e-19			5.5200e-22
69	350.00		3.0000e-22			3.3000e-19			7.8900e-22
70	345.00		5.0000e-22			3.3000e-19			1.1300e-21
71	340.00		7.0000e-22			3.2000e-19			1.6100e-21
72	335.00		9.0000e-22			3.1000e-19			2.3000e-21
73	330.00		1.2000e-21			2.8000e-19			3.2900e-21
74	325.00		1.5000e-21			2.5000e-19			4.7000e-21
75	320.00		2.0000e-21			2.4000e-19			6.7100e-21
76	315.00		2.8000e-21			2.2000e-19			9.5900e-21
77	310.00		3.7000e-21			1.8000e-19			1.3700e-20
78	305.33		4.9000e-21			1.6000e-19			1.9100e-20
79	300.73		6.6100e-21			1.2000e-19			2.6500e-20
80	296.28		8.0500e-21			9.0000e-20			3.6500e-20
81	292.00		9.9000e-21			7.0000e-20			4.9500e-20
82	287.78		1.2800e-20			6.0000e-20			6.6900e-20
83	283.69		1.6100e-20			5.3000e-20			8.9500e-20
84	279.74		2.0000e-20			4.8000e-20			1.1800e-19
85	275.89		2.4000e-20			4.2000e-20			1.2700e-19
86	272.14		2.8800e-20	1.2600e-19		3.5000e-20			1.4400e-19
87	268.50		3.5400e-20	1.5000e-19		2.7000e-20			1.6800e-19
88	264.94		4.2000e-20	1.7400e-19		2.1000e-20			2.0000e-19
89	261.44		4.7800e-20	2.0000e-19		2.0000e-20			2.4300e-19
90	258.04		5.7500e-20	2.5100e-19		1.7000e-20			2.8000e-19
91	254.79		6.8000e-20	3.4500e-19		1.6000e-20			3.2400e-19
92	251.59		7.9500e-20	4.2500e-19		2.4000e-20			3.6900e-19
93	248.44		8.8000e-20	5.9000e-19		3.3000e-20			4.4000e-19
94	245.39		9.9000e-20	8.3000e-19		4.3000e-20			5.0200e-19
95	242.44		1.1200e-19	1.0400e-18		5.0000e-20			5.6000e-19
96	239.54		1.2700e-19	1.2500e-18	4.0000e-24	7.0000e-20			6.3500e-19
97	236.69		1.3800e-19	1.7300e-18	6.6000e-24	1.0000e-19			7.2000e-19
98	233.94		1.5200e-19	2.0900e-18	1.2000e-23	1.6000e-19			8.1000e-19
99	231.24		1.7000e-19	2.4300e-18	2.3000e-23	2.2000e-19			9.0000e-19
100	228.59		1.9900e-19	2.8900e-18	4.4000e-23	2.5000e-19			1.0900e-18
101	226.00		2.0800e-19	3.3200e-18	8.2000e-23	2.8000e-19			1.3000e-18
102	223.44		2.2600e-19	3.6600e-18	1.7000e-22	3.4000e-19			1.6300e-18
103	221.00		2.4700e-19	3.8800e-18	2.7000e-22	3.8000e-19			2.0000e-18
104	218.59		2.6500e-19	4.2200e-18	5.2000e-22	4.0000e-19			2.5000e-18
105	216.19		2.9000e-19	4.4600e-18	9.1000e-22	4.2000e-19			3.2000e-18
106	213.89		3.1000e-19	4.6700e-18	1.7000e-21	4.1000e-19			3.9500e-18
107	211.64		3.4700e-19	4.8100e-18	3.1000e-21	3.9000e-19			4.7000e-18
108	209.39		3.5400e-19	4.9200e-18	5.4000e-21	3.9000e-19			5.8000e-18
109	207.24		3.7600e-19	4.9400e-18	8.3000e-21	3.9000e-19			7.0500e-18
110	205.15		3.9400e-19	4.9300e-18	1.2700e-20	3.6300e-19			8.0000e-18

bin	wlc	h2o	h2o2	hoo	n2o	no2	no3=no2+o	no3=no+o2	n2o5
111	203.05		4.2700e-19	4.9100e-18	1.8200e-20	3.1500e-19			8.5000e-18
112	201.00		4.8000e-19	4.8500e-18	2.4200e-20	2.7400e-19			9.0000e-18
113	199.00	1.0700e-22	4.9100e-19	4.7800e-18	3.5000e-20	2.3700e-19			
114	197.05	2.4200e-22	5.2600e-19	4.6900e-18	4.8600e-20	2.2900e-19			
115	195.15	5.1200e-22	5.6100e-19	4.6100e-18	6.0800e-20	2.3200e-19			
116	193.25	1.2100e-21	5.9800e-19	4.4900e-18	7.3400e-20	2.4500e-19			
117	191.40	2.9000e-21	6.4000e-19	4.3600e-18	8.6000e-20	2.8000e-19			
118	189.60	5.9500e-21	6.8200e-19		1.0100e-19				
119	187.80	1.2000e-20	8.5600e-19		1.1300e-19				
120	186.05	2.6200e-20	8.9400e-19		1.1800e-19				
121	184.35	7.0000e-20	9.1600e-19		1.2700e-19				
122	182.65	1.8600e-19	9.3800e-19		1.3300e-19				
123	181.00	4.5500e-19	1.0300e-18		1.3500e-19				
124	179.40	1.2000e-18	1.1700e-18						
125	177.80	1.8800e-18	1.4000e-18						
126	176.20	2.4000e-18	1.5500e-18						
127	174.65	2.9000e-18							
128	173.15	3.4000e-18							
129	170.94	4.0000e-18							
130	168.09	4.6000e-18							
131	165.29	4.8000e-18							
132	162.59	4.1500e-18							
133	160.00	3.5000e-18							
134	157.44	2.8000e-18							
135	155.00	2.2000e-18							
136	152.64	1.4800e-18							
137	150.34	1.0000e-18							
138	148.09	5.8000e-19							
139	145.94	5.0000e-19							
140	143.84	5.1000e-19							
141	141.79	5.8000e-19							
142	139.84	7.0000e-19							
143	138.40	1.0300e-18							
144	137.45	1.4500e-18							
145	136.50	2.0300e-18							
146	135.55	2.7000e-18							
147	134.65	3.4000e-18							
148	133.75	4.1000e-18							

bin	wlc	hno2	hno3	hno4	hcl	hocl	clo	clono	clono2
57	410.00					4.0000e-22			
58	405.00					4.5000e-22			
59	400.00					5.7000e-22		6.0000e-21	5.5000e-22
60	395.00					1.0000e-21		1.5000e-20	7.0000e-22
61	390.00	1.0000e-20				1.4000e-21		2.2000e-20	8.5000e-22
62	385.00	1.3300e-19				1.9000e-21		3.3000e-20	9.8000e-22
63	380.00	9.7000e-20				2.5000e-21		4.1500e-20	1.1500e-21
64	375.00	3.1000e-20				3.3000e-21		6.9000e-20	1.3000e-21
65	370.00	1.7000e-19				4.0000e-21		8.9000e-20	1.4000e-21
66	365.00	2.1800e-19				6.1000e-21		1.1100e-19	1.6000e-21
67	360.00	7.3000e-20				7.8000e-21		1.6200e-19	1.7000e-21
68	355.00	2.3800e-19				1.0500e-20		2.2600e-19	1.8000e-21
69	350.00	1.5000e-19				1.3500e-20		2.6200e-19	2.0000e-21
70	345.00	1.1800e-19				1.7500e-20		3.4400e-19	2.2000e-21
71	340.00	1.5700e-19				2.3000e-20		4.4100e-19	2.5000e-21
72	335.00	7.1000e-20				2.9000e-20		5.6300e-19	2.9000e-21
73	330.00	8.6000e-20	2.0000e-23	1.0000e-21		3.5000e-20		5.9000e-19	3.5000e-21
74	325.00	4.2000e-20	5.0000e-23	2.0000e-21		4.3000e-20		7.5000e-19	4.6000e-21
75	320.00	4.0000e-20	1.2000e-22	3.0000e-21		5.1000e-20		8.1000e-19	6.3000e-21
76	315.00	7.3000e-21	3.2000e-22	4.5000e-21		5.6000e-20		9.7500e-19	8.9000e-21
77	310.00	1.2000e-21	7.1000e-22	7.3000e-21		6.1000e-20		1.0500e-18	1.2800e-20
78	305.33		1.4000e-21	1.1000e-20		6.1000e-20	2.0000e-19	1.1100e-18	1.7000e-20
79	300.73		2.3000e-21	1.6000e-20		6.0000e-20	3.6000e-19	1.2800e-18	2.4000e-20
80	296.28		3.6500e-21	2.3000e-20		5.9000e-20	7.2000e-19	1.4100e-18	3.4000e-20
81	292.00		5.2000e-21	3.4000e-20		5.5000e-20	1.3000e-18	1.4400e-18	4.6000e-20
82	287.78		7.0700e-21	5.0000e-20		5.1000e-20	1.9000e-18	1.4500e-18	6.6000e-20
83	283.69		9.4412e-21	7.1000e-20		4.9000e-20	2.2500e-18	1.4600e-18	8.6000e-20
84	279.74		1.1531e-20	9.4000e-20		4.8000e-20	2.5500e-18	1.3200e-18	1.0500e-19
85	275.89		1.3556e-20	1.3000e-19		5.1000e-20	5.0000e-18	1.1300e-18	1.3000e-19
86	272.14		1.5345e-20	1.6000e-19		5.7000e-20	5.1000e-18	9.7000e-19	1.6000e-19
87	268.50		1.6805e-20	1.9000e-19		5.6000e-20	5.3000e-18	8.0000e-19	2.0000e-19
88	264.94		1.8019e-20	2.2000e-19		8.0000e-20	5.4000e-18	7.0000e-19	2.3000e-19
89	261.44		1.8856e-20	2.6000e-19		1.0000e-19	5.5301e-18	6.6000e-19	2.8000e-19
90	258.04		1.9196e-20	3.1000e-19		1.1500e-19	4.9862e-18	6.4000e-19	3.3000e-19
91	254.79		1.9400e-20	3.5000e-19		1.4000e-19	4.4622e-18	6.6000e-19	4.0000e-19
92	251.59		1.9400e-20	4.0000e-19		1.6500e-19	3.8862e-18	8.2000e-19	4.5000e-19
93	248.44		1.9812e-20	4.4000e-19		1.9000e-19	3.3192e-18	1.1700e-18	5.6000e-19
94	245.39		2.0726e-20	4.9000e-19		2.1000e-19	2.7625e-18	1.3500e-18	6.6000e-19
95	242.44		2.2770e-20	5.4000e-19		2.2000e-19	2.1930e-18	1.5800e-18	8.0000e-19
96	239.54		2.6824e-20	5.9000e-19		2.2000e-19	1.8450e-18	1.7700e-18	9.9000e-19
97	236.69		3.2632e-20	6.4000e-19		2.1000e-19	1.4523e-18	2.0500e-18	1.2500e-18
98	233.94		4.0698e-20	7.1000e-19		2.0000e-19	1.2048e-18	2.2000e-18	1.5000e-18
99	231.24		5.0465e-20	7.7000e-19		1.9000e-19	9.0214e-19		1.8500e-18
100	228.59		6.3279e-20	8.5000e-19		1.8000e-19	7.9088e-19		2.2000e-18

bin	wlc	hno2	hno3	hno4	hcl	hocl	clo	clono	clono2
101	226.00		7.7851e-20	9.1000e-19		1.6000e-19	6.8170e-19		2.7000e-18
102	223.44		9.5685e-20	1.0000e-18		1.4000e-19	5.4000e-19		3.2000e-18
103	221.00		1.2712e-19	1.1000e-18		1.2000e-19	4.8000e-19		3.4000e-18
104	218.59		1.7335e-19	1.3000e-18	7.0000e-22	1.0000e-19			3.5000e-18
105	216.19		2.6474e-19	1.5000e-18	1.1400e-21	8.6000e-20			3.5000e-18
106	213.89		4.2054e-19	1.8000e-18	1.8000e-21	7.5000e-20			3.5000e-18
107	211.64		6.7985e-19	2.1000e-18	3.0000e-21	6.5000e-20			3.4000e-18
108	209.32		1.0735e-18	2.5000e-18	4.6000e-21	6.0000e-20			3.3000e-18
109	207.24		1.6820e-18	2.9000e-18	7.0000e-21	5.8000e-20			3.2000e-18
110	205.15		2.7300e-18	3.7700e-18	1.0000e-20	5.5500e-20			3.0000e-18
111	203.05		4.2000e-18	4.[illegible]000e-18	1.6100e-20	5.3100e-20			2.9000e-18
112	201.00		5.7700e-18	5.2100e-18	2.3800e-20	5.1500e-20			2.9000e-18
113	199.00		7.5200e-18	[illegible].1200e-18	3.0900e-20				3.0000e-18
114	197.05		9.9400e-18	7.4500e-18	4.2100e-20				3.2000e-18
115	195.15		1.1300e-17	8.2000e-18	6.2000e-20				3.5000e-18
116	193.25		1.2800e-17	8.9000e-18	8.7300e-20				4.0000e-18
117	191.40		1.4400e-17	9.6000e-18	1.2400e-19				4.7000e-18
118	189.60		1.5700e-17		1.5900e-19				
119	187.80		1.5800e-17		2.1100e-19				
120	186.05				2.7900e-19				
121	184.35				3.5000e-19				
122	182.65				4.2300e-19				
123	181.00				5.1800e-19				
124	179.40				6.5200e-19				
125	177.80				8.4000e-19				
126	176.20				1.0400e-18				
127	174.65				1.1200e-18				
128	173.15				1.3000e-18				
129	170.94				1.5400e-18				
130	168.09				1.9600e-18				
131	165.29				2.4200e-18				
132	162.59				2.8900e-18				
133	160.00				3.3200e-18				
134	157.44				3.6400e-18				
135	155.00				3.8200e-18				
136	152.64				3.6800e-18				
137	150.34				3.5000e-18				
138	148.09				3.2400e-18				
139	145.94				2.9400e-18				
140	143.84				2.6500e-18				
141	141.79				2.3500e-18				
142	139.84				2.0800e-18				

bin	wlc	ch3cl	ch3ccl3	ccl4	cfcl3	cf2cl2	cf3cl	chfcl2	chf2cl
88	264.94			1.2300e-22					
89	261.44			1.7000e-22					
90	258.04			3.5300e-22					
91	254.79			7.0000e-22					
92	251.59			1.3200e-21					
93	248.44			2.1800e-21					
94	245.39			3.2700e-21	1.5000e-22				
95	242.44			5.1500e-21	2.6000e-22				
96	239.54		3.7000e-22	8.4000e-21	4.9000e-22				
97	236.69		7.5000e-22	1.3500e-20	9.3000e-22				
98	233.94		1.4800e-21	2.1600e-20	1.5300e-21				
99	231.24		2.8600e-21	3.3300e-20	2.5800e-21				
100	228.59		5.0400e-21	5.0500e-20	4.5000e-21				
101	226.00		9.1800e-21	7.1000e-20	7.0500e-21			1.3000e-22	
102	223.44		1.5800e-20	1.0700e-19	1.2800e-20			2.6000e-22	
103	221.00		2.6300e-20	1.4800e-19	1.9300e-20			5.2000e-22	
104	218.59		4.2700e-20	1.9800e-19	3.0000e-20	4.6000e-22		9.4000e-22	7.0000e-24
105	216.19	3.0000e-22	7.0600e-20	2.7700e-19	5.5000e-20	8.6000e-22		1.5000e-21	1.2000e-23
106	213.89	6.1000e-22	1.1400e-19	3.5000e-19	8.3000e-20	1.5300e-21		2.5000e-21	2.0000e-23
107	211.64	1.1400e-21	1.7900e-19	4.2000e-19	1.3000e-19	2.8000e-21		4.1000e-21	3.4000e-23
108	209.39	2.0600e-21	2.5700e-19	4.8000e-19	1.7900e-19	5.4000e-21		7.5000e-21	6.4000e-23
109	207.24	3.5500e-21	3.5500e-19	5.3000e-19	2.4000e-19	9.7000e-21		1.3000e-20	8.5000e-23
110	205.15	5.6000e-21	4.4000e-19	5.9000e-19	3.4500e-19	1.7100e-20	4.0000e-23	2.2000e-20	1.2300e-22
111	203.05	8.5000e-21	5.8000e-19	6.2000e-19	4.5400e-19	2.9800e-20	6.4000e-23	3.4000e-20	1.8800e-22
112	201.00	1.4000e-20	7.3000e-19	6.5000e-19	5.7100e-19	4.8000e-20	1.0000e-22	4.8000e-20	2.8700e-22
113	199.00	2.1000e-20	8.9500e-19	6.7000e-19	7.1800e-19	7.8000e-20	[illegible]	7.1000e-20	4.2200e-22
114	197.05	3.2000e-20	1.0800e-18	6.8000e-19	9.0000e-19	1.2600e-19	2.6100e-22	1.0800e-19	6.3000e-22
115	195.15	4.6000e-20	1.2800e-18	7.1000e-19	1.0900e-18	1.9800e-19	4.2300e-22	1.5700e-19	9.1000e-22
116	193.25	7.0000e-20	1.5200e-18	7.6000e-19	1.3000e-18	2.9200e-19	6.1700e-22	2.4900e-19	1.3400e-21
117	191.40	1.0100e-19	1.8000e-18	1.0100e-18	1.5700e-18	4.4000e-19	8.8400e-22	3.4900e-19	1.9900e-21
118	189.60	1.3700e-19	2.0300e-18	1.5400e-18	1.8100e-18	6.0000e-19	1.2300e-21	4.8000e-19	2.9000e-21
119	187.80	1.8000e-19	2.2400e-18	2.1200e-18	2.1000e-18	8.0000e-19	1.6000e-21	6.4500e-19	4.2500e-21
120	186.05	2.4300e-19	2.6700e-18	3.0100e-18	2.3300e-18	1.0400e-18	2.0700e-21	8.3000e-19	6.2700e-21
121	184.35			4.3900e-18	2.5800e-18	1.3200e-18	2.6100e-21		8.7000e-21
122	182.65			5.2700e-18	2.7700e-18	1.5600e-18	3.2200e-21		1.1900e-20
123	181.00			6.8000e-18	3.0000e-18	1.8100e-18			1.7000e-20
124	179.40			8.5500e-18	3.1000e-18	2.0600e-18			2.3500e-20
125	177.80			9.7000e-18	3.1000e-18	2.2200e-18			3.1600e-20
126	176.20			1.0400e-17	3.1000e-18	2.2600e-18			4.3800e-20
127	174.65			9.9000e-18	3.1500e-18				5.7000e-20
128	173.15				3.2000e-18				7.4000e-20
129	170.94				3.2000e-18				1.1000e-19
130	168.09				3.1000e-18				1.8000e-19
131	165.29								3.2000e-19
132	162.59								5.5000e-19
133	160.00								9.0000e-19
134	157.44								1.2000e-18

bin	wlc	cfcl2cfcl2	cf2clcfcl2	cf2clcf2cl	cf3cf2cl	ch3cf2cl	ocs	so2
81	292.00						1.4400e-24	
82	287.78						3.8000e-24	
83	283.69						6.4800e-24	
84	279.74						1.5100e-23	
85	275.89						3.4800e-23	
86	272.14						7.2700e-23	
87	268.50						1.4300e-22	
88	264.94						3.0200e-22	
89	261.44						6.4800e-22	
90	258.04						1.2800e-21	
91	254.79						2.5400e-21	
92	251.59						4.8900e-21	
93	248.44						9.2900e-21	
94	245.39						1.6500e-20	
95	242.44						2.8000e-20	
96	239.54						4.4900e-20	
97	236.69						7.0000e-20	
98	233.94	2.9000e-22	1.4500e-22				1.0100e-19	
99	231.24	4.6000e-22	2.3000e-22				1.3500e-19	
100	228.59	7.8000e-22	3.9000e-22				1.7100e-19	
101	226.00	1.4000e-21	7.0000e-22				1.9700e-19	
102	223.44	2.2000e-21	1.1000e-21				2.1200e-19	
103	221.00	3.6000e-21	1.8000e-21	7.0000e-23			2.1200e-19	
104	218.59	5.8000e-21	2.9000e-21	1.1500e-22			1.9900e-19	4.6200e-19
105	216.19	9.4000e-21	4.7000e-21	2.2200e-22			1.8200e-19	6.2500e-19
106	213.89	1.5600e-20	7.8000e-21	4.3000e-22			1.5700e-19	8.1000e-19
107	211.64	2.5200e-20	1.2600e-20	6.3000e-22		1.4000e-22	1.2700e-19	1.0100e-18
108	209.39	4.1000e-20	2.0500e-20	1.1000e-21		2.2000e-22	1.0200e-19	1.2800e-18
109	207.24	6.4000e-20	3.2000e-20	1.8000e-21	1.1000e-22	3.6000e-22	7.8500e-20	1.5500e-18
110	205.15	9.4000e-20	4.7000e-20	3.0000e-21	1.8000e-22	5.0000e-22	5.9500e-20	1.8700e-18
111	203.05	1.4000e-19	7.0000e-20	4.4000e-21	2.7000e-22	7.4000e-22	4.4400e-20	2.2000e-18
112	201.00	2.0800e-19	1.0400e-19	6.7000e-21	4.1000e-22	1.2000e-21	3.2400e-20	2.5100e-18
113	199.00	2.9800e-19	1.4900e-19	1.0000e-20	6.6000e-22	1.7000e-21	2.3800e-20	2.8200e-18
114	197.05	4.2600e-19	2.1300e-19	1.5400e-20	9.3000e-22	2.3000e-21	1.7600e-20	3.1400e-18
115	195.15	6.0000e-19	3.0000e-19	2.5200e-20	1.4000e-21	3.2000e-21	1.3200e-20	3.4300e-18
116	193.25	8.2000e-19	4.1000e-19	3.1300e-20	2.0000e-21	5.2000e-21	1.1000e-20	3.6900e-18
117	191.40	1.0760e-18	5.3800e-19	4.4400e-20	2.7000e-21	7.9000e-21	1.1600e-20	3.7500e-18
118	189.60	1.3780e-18	6.8900e-19	5.9700e-20	3.6000e-21	1.1500e-20	1.8000e-20	3.6000e-18
119	187.80	1.7000e-18	8.5000e-19	7.9100e-20	4.9000e-21	1.6000e-20	4.0500e-20	3.3000e-18
120	186.05	2.1000e-18	1.0500e-18	1.0000e-19	6.1000e-21	2.2000e-20	9.3600e-20	2.9800e-18

bin	wlc	ch2o=cho+h [b]	ch2o=co+h2 [b]	ch3ooh	cl2	cloo
49	450.00				3.4026e-21	
50	445.00				4.3028e-21	
51	440.00				5.3028e-21	
52	435.00				6.0037e-21	
53	430.00				7.3038e-21	
54	425.00				8.3545e-21	
55	420.00				9.9046e-21	
56	415.00				1.0009e-20	
57	410.00				1.3009e-20	
58	405.00				1.2022e-20	
59	400.00				1.9022e-20	
60	395.00				2.5025e-20	
61	390.00				3.3026e-20	
62	385.00				3.2056e-20	
63	380.00				4.9056e-20	
64	375.00				5.9080e-20	
65	370.00				8.3081e-20	
66	365.00				1.0210e-19	
67	360.00		4.0000e-24		1.3110e-19	
68	355.00		8.5000e-22		1.6558e-19	
69	350.00		3.8400e-22	4.0000e-22	1.8908e-19	
70	345.00		1.7120e-21	5.1000e-22	2.2604e-19	
71	340.00	3.1000e-23	6.1800e-21	6.6000e-22	2.3604e-19	
72	335.00	1.4500e-22	7.1200e-22	8.7000e-22	2.6596e-19	
73	330.00	3.1500e-21	5.7700e-21	1.1000e-21	2.5596e-19	
74	325.00	6.6000e-21	7.0600e-21	1.5000e-21	2.6140e-19	
75	320.00	7.4800e-21	4.8000e-21	2.0000e-21	2.3590e-19	
76	315.00	1.8910e-20	8.0700e-21	2.6000e-21	2.1737e-19	
77	310.00	1.1820e-20	3.7100e-21	3.5000e-21	1.8487e-19	
78	305.33	2.8630e-20	7.5700e-21	4.5000e-21	1.5466e-19	
79	300.73	1.1720e-20	3.0000e-21	5.5000e-21	1.2403e-19	
80	296.28	2.0810e-20	5.8700e-21	6.7000e-21	9.9557e-20	
81	292.00	1.5490e-20	5.6100e-21	8.4000e-21	7.2543e-20	
82	287.78	1.3260e-20	6.1600e-21	1.0000e-20	5.6583e-20	
83	283.69	1.4050e-20	8.4600e-21	1.2500e-20	3.3710e-20	
84	279.74	9.1100e-21	7.5400e-21	1.6000e-20	2.6522e-20	
85	275.89	8.3100e-21	9.5300e-21	1.9000e-20	1.9515e-20	
86	272.14	4.2300e-21	7.2600e-21	2.3000e-20	1.0189e-20	
87	268.50	2.7700e-21	7.1200e-21	2.7000e-20	7.8169e-21	5.7655e-18
88	264.94	1.0100e-21	4.3700e-21	3.2000e-20	2.8432e-21	7.3334e-18
89	261.44	6.6100e-22	3.6600e-21	3.6000e-20	2.4582e-21	9.3098e-18
90	258.04	6.6900e-22	4.0400e-21	4.1000e-20	2.0843e-21	1.0941e-17
91	254.79			4.7000e-20	1.3916e-21	1.2438e-17
92	251.59			5.4000e-20	1.2636e-21	1.3491e-17
93	248.44			6.3000e-20	1.1376e-21	1.3113e-17
94	245.39			7.1000e-20	1.0156e-21	1.2872e-17
95	242.44			8.1000e-20	8.9767e-22	1.1819e-17
96	239.54			9.3000e-20	7.8168e-22	1.0253e-17
97	236.69			1.0500e-19		8.7814e-18
98	233.94			1.1700e-19		7.1863e-18
99	231.24			1.3000e-19		5.4711e-18
100	228.59			1.4500e-19		4.2525e-18

bin	wlc	ch2o=cho+h	ch2o=co+h2	ch3ooh	cl2	cloo
101	226.00			1.6500e-19		3.0568e-18
102	223.44			1.9000e-19		
103	221.00			2.0500e-19		
104	218.59			2.4000e-19		
105	216.19			2.7000e-19		
106	213.89			3.0000e-19		
107	211.64			3.4000e-19		
108	209.39			3.8000e-19		

a. Ozone effective photolytic cross sections at top of model altitude range (55 km).
b. Formaldehyde effective photolytic cross sections at the surface (0 km).

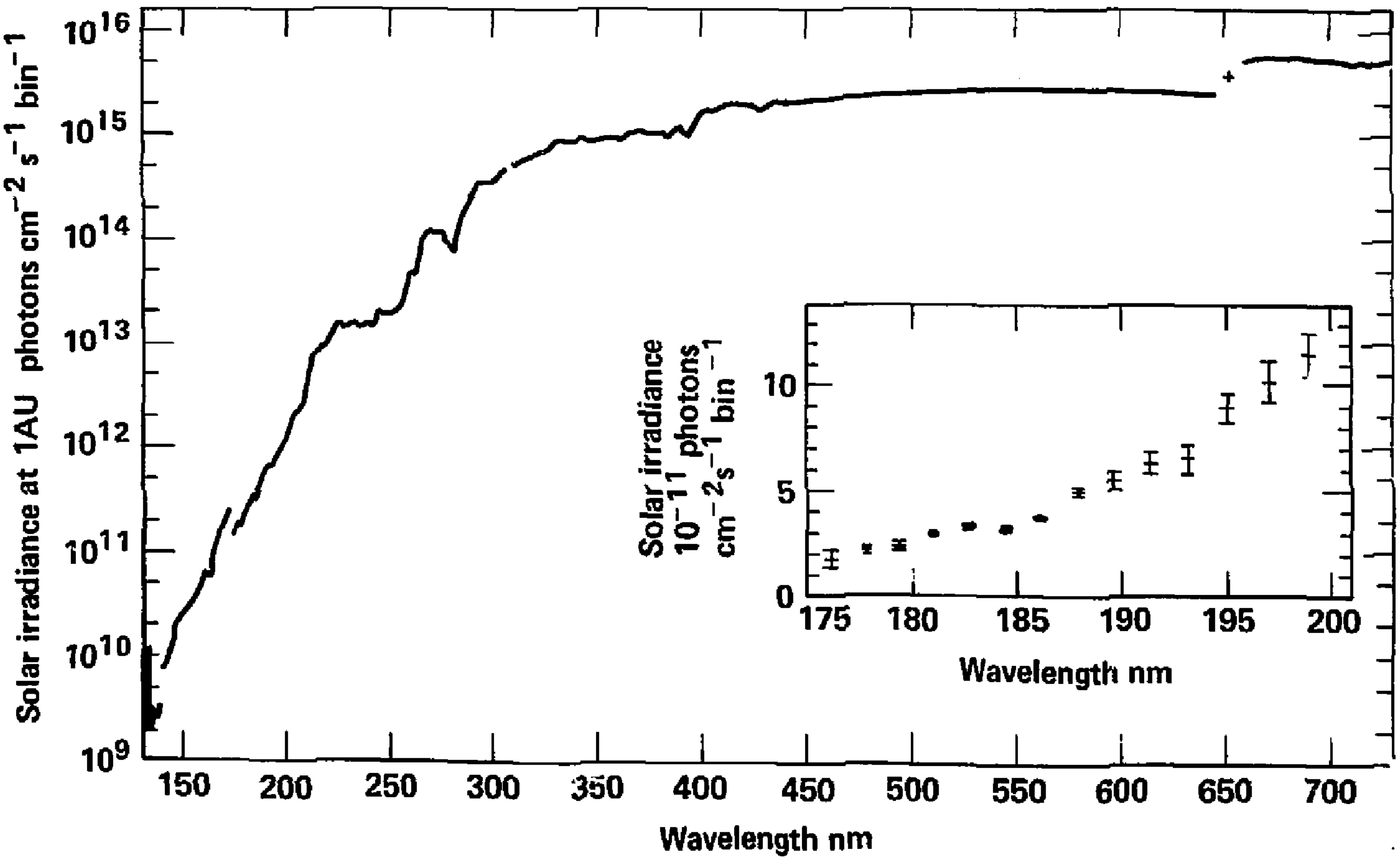

Figure 1. Solar flux above the atmosphere. Discontinuities correspond to changes in bin width. Inset shows far uv variability with solar activity (WMO, 1982).

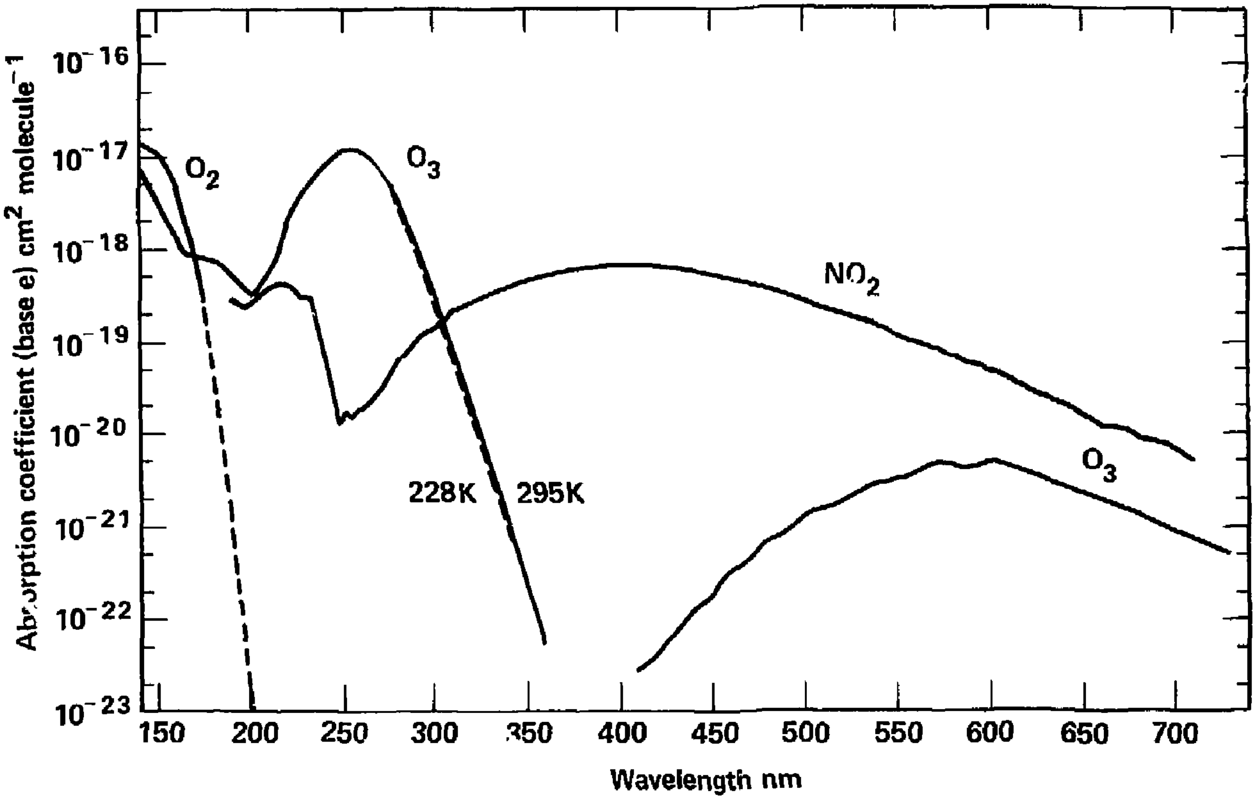

Figure 2. Spectra of gases that control transmission in the atmosphere. Dashed line for O_2 corresponds to Schumann-Runge bands in which effective absorption coefficients depend on altitude and solar zenith angle.

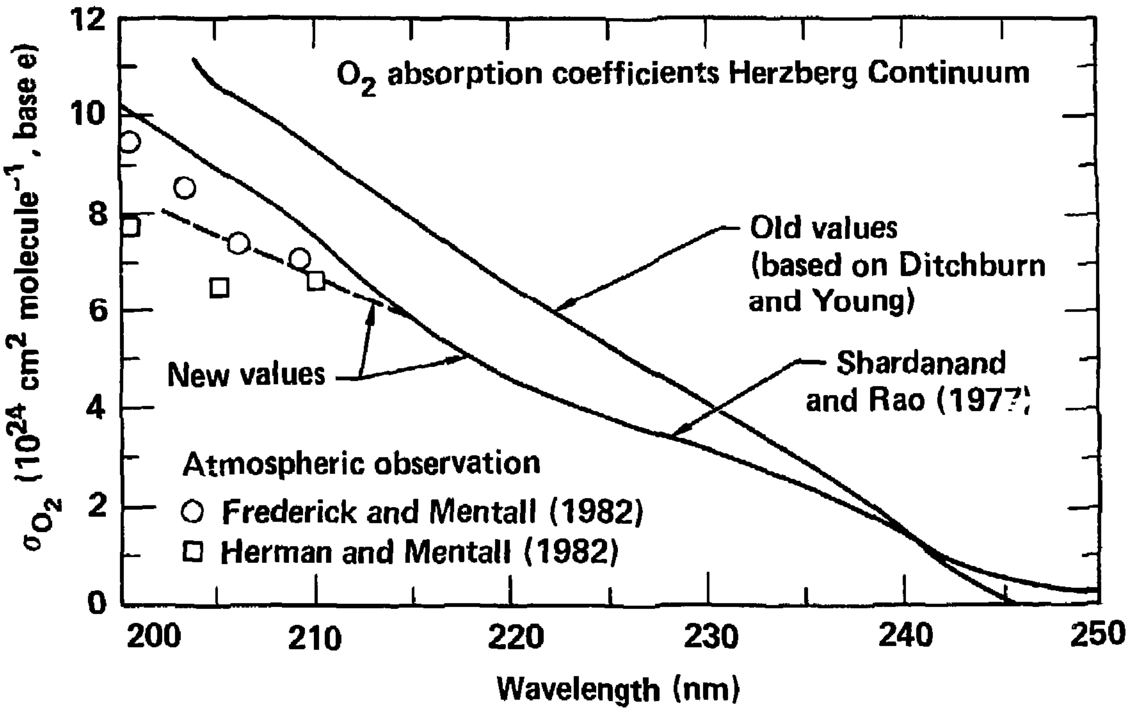

Figure 3. O_2 Herzberg continuum region.

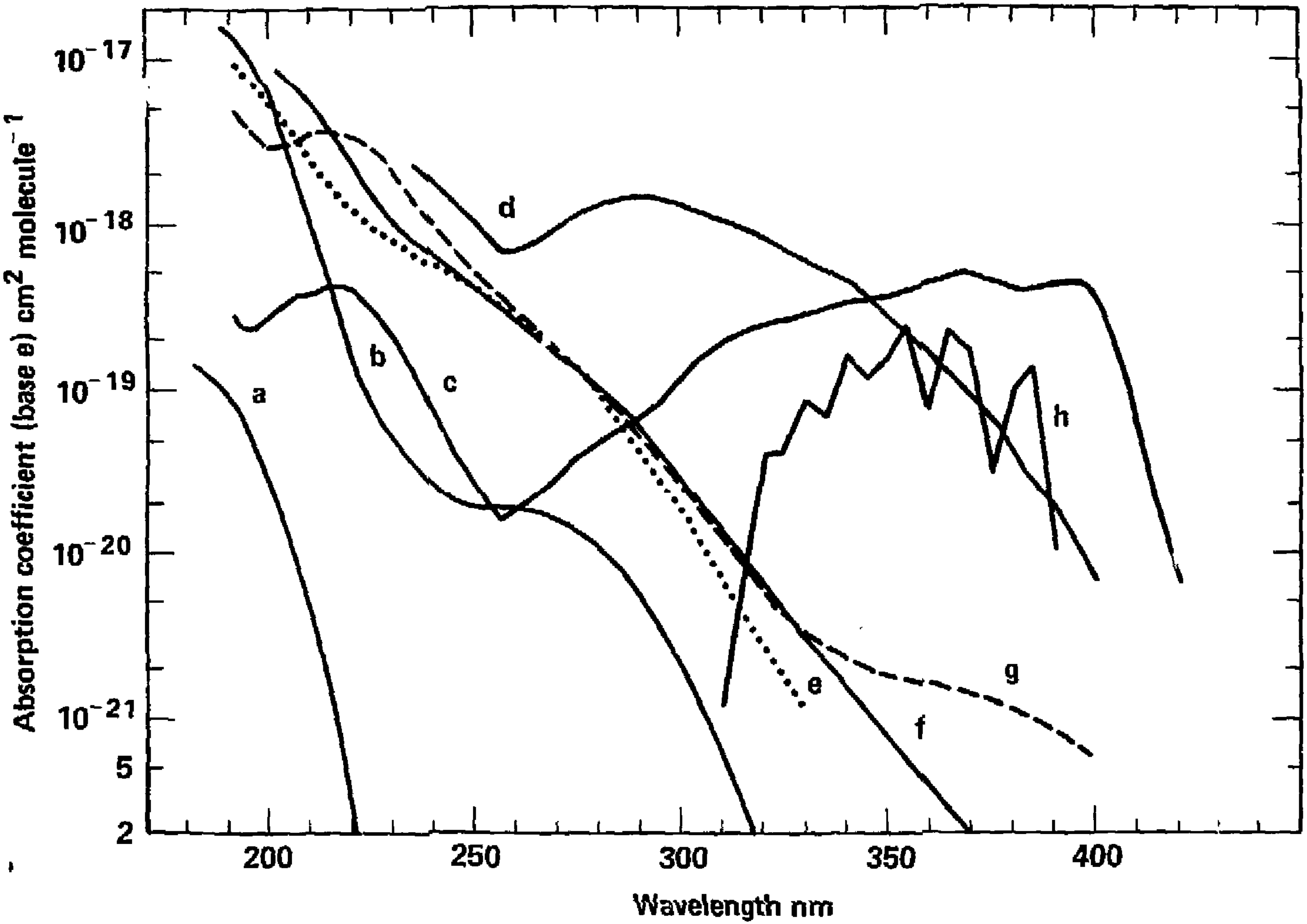

Figure 4. NO_x absorption coefficients: a) N_2O, b) HNO_3, c) NO_2, d) ClONO, e) $HOONO_2$, f) N_2O_5, g) $ClONO_2$, h) HONO.

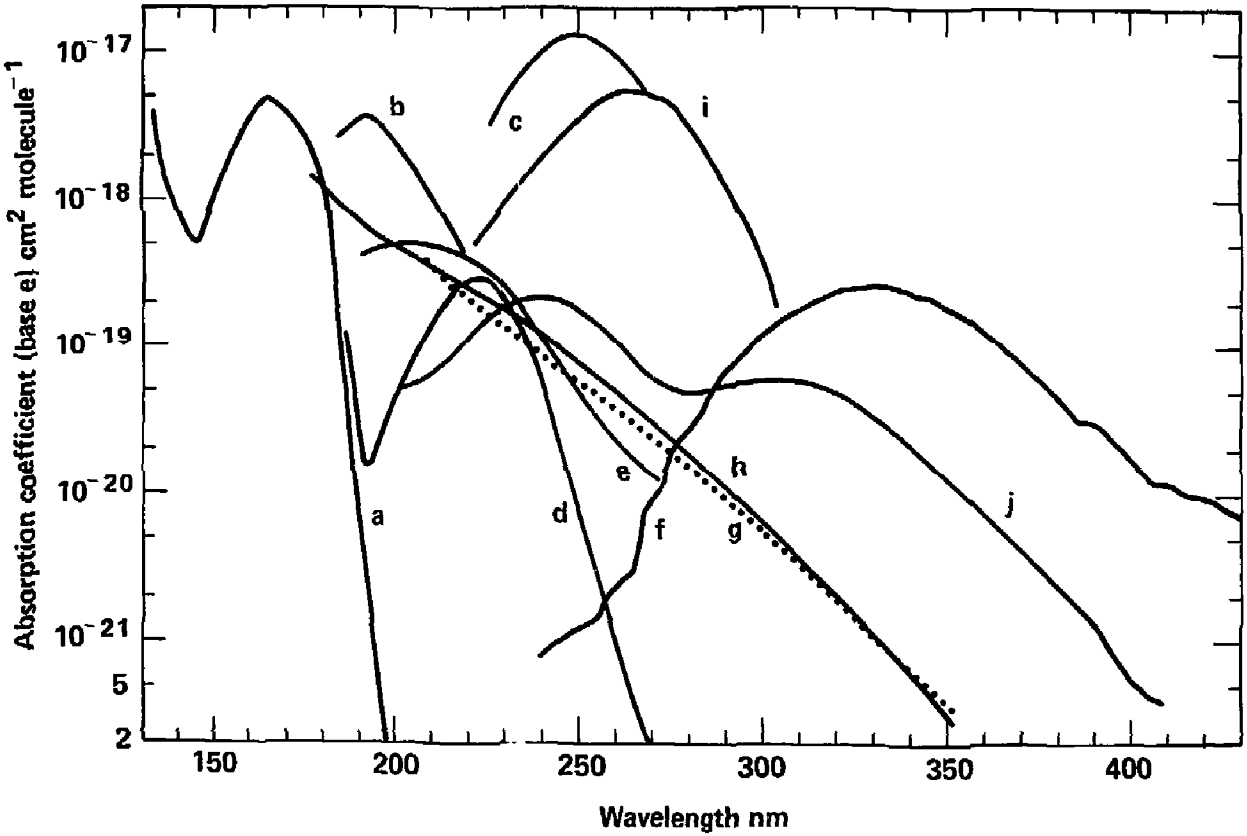

Figure 5. HO_x, ClO_x, and sulfur species' absorption coefficients; a) H_2O, b) SO_2, c) ClOO, d) OCS, e) HOO, f) Cl_2, g) CH_3OOH, h) H_2O_2, i) ClO, j) HOCl.

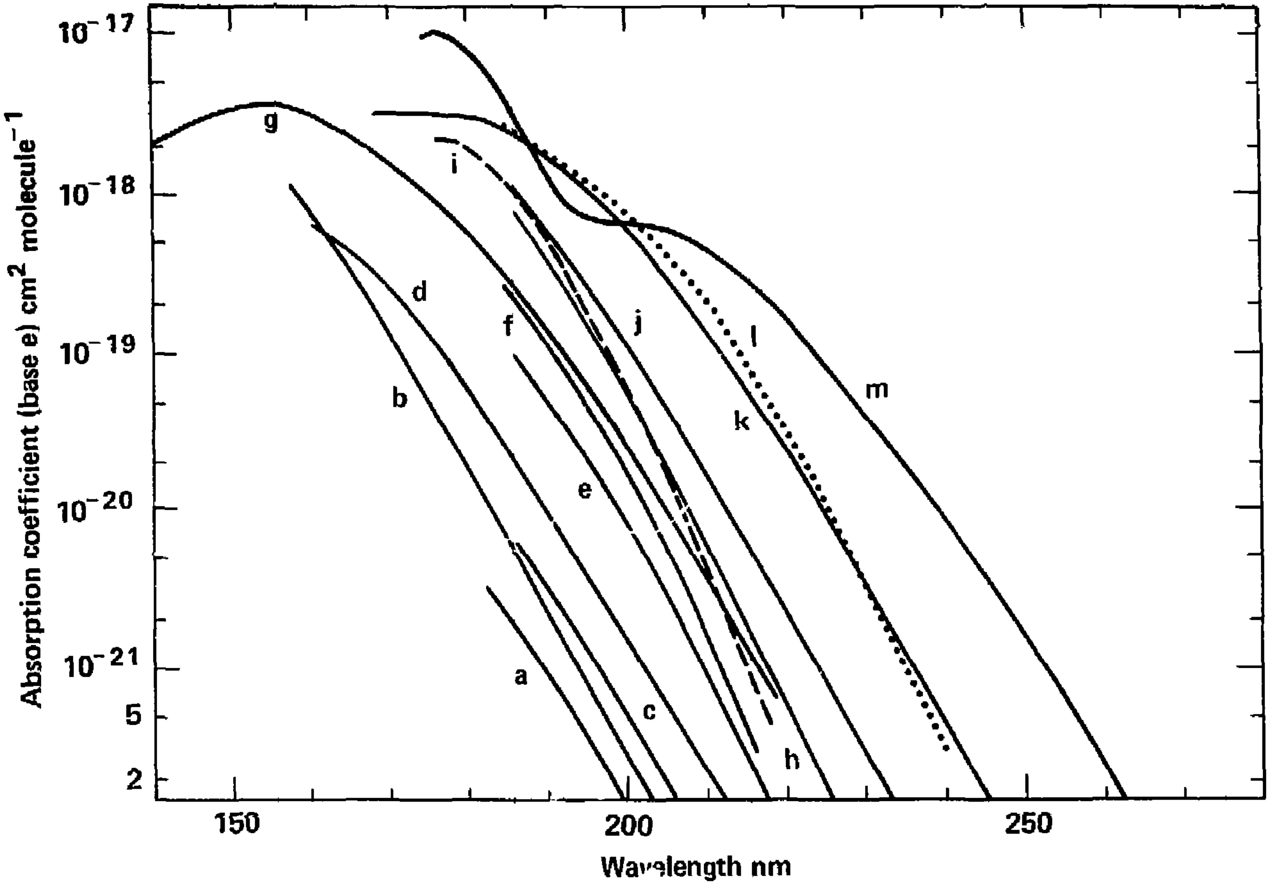

Figure 6. Chlorocarbon and HCl absorption coefficients; a) $CFCl_3$ (CFC-13), b) CHF_2Cl (CFC-22), c) CF_3CF_2Cl (CFC-115), d) CH_3CF_2Cl (CFC-142b), e) CF_2ClCF_2Cl (CFC-114), f) CH_3Cl, g) HCl, h) $CHFCl_2$ (CFC-21), i) CF_2Cl_2 (CFC-12), j) $CFCl_2CF_2Cl$ (CFC-113), k) C [illegible]$_3$ (CFC-11), l) CH_3CCl_3, m) CCl_4.

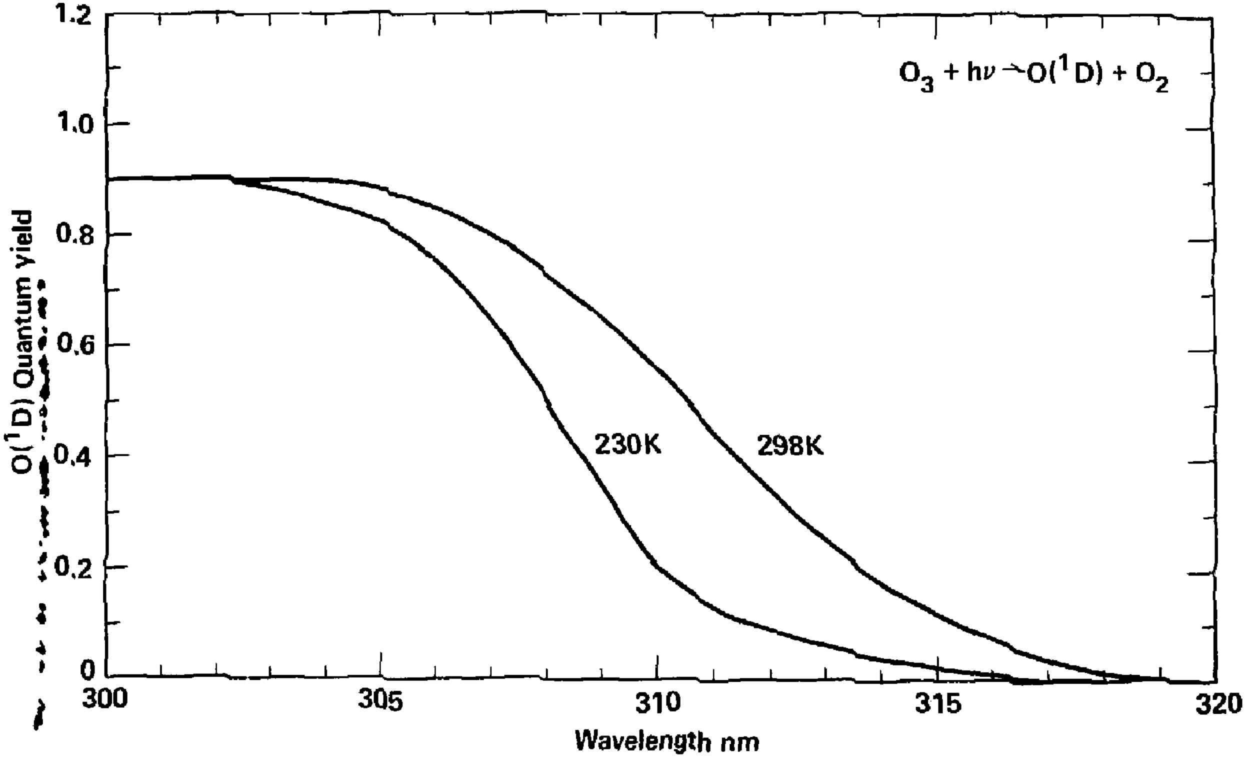

Figure 7. Qantum yield for $O(^1D)$ production in O_3 photolysis.

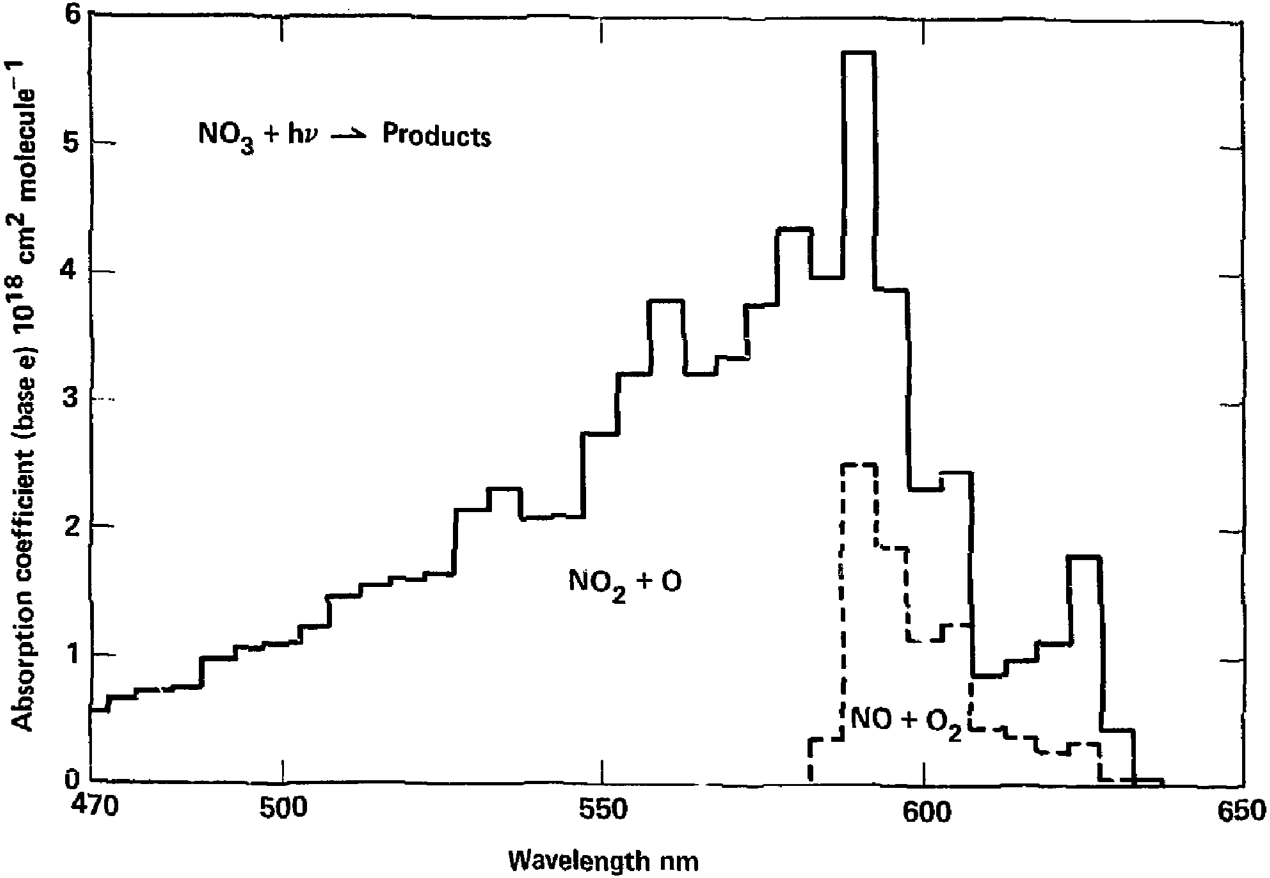

Figure 8. Fffective absorption coefficients ($\sigma\phi$) for the two channels in NO_3 photolysis.

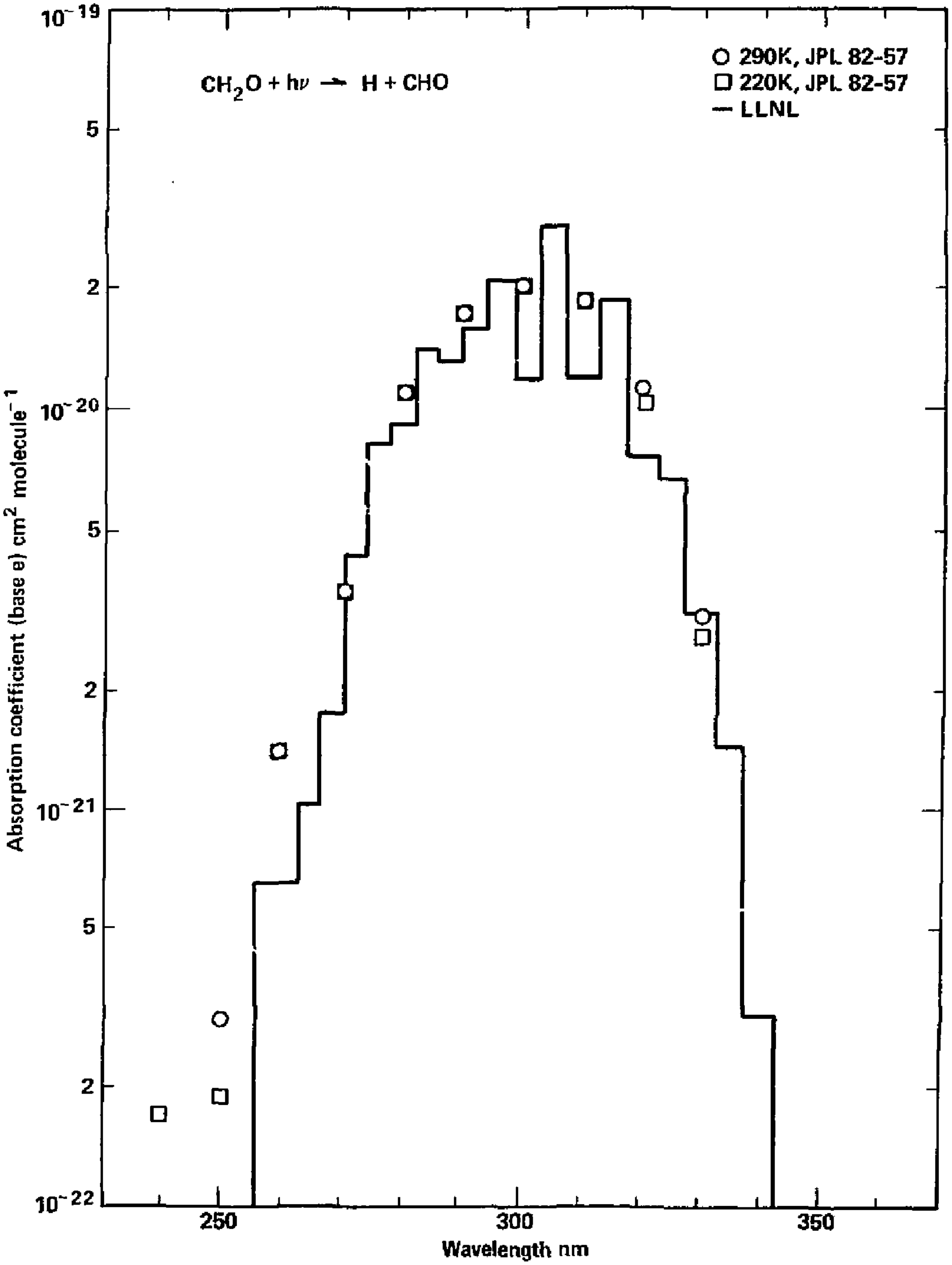

Figure 9. Effective absorption coefficients for radical products (H + CHO) in CH_2O photolysis. NASA recommended values (DeMore et al., 1982) at two temperatures are also shown.

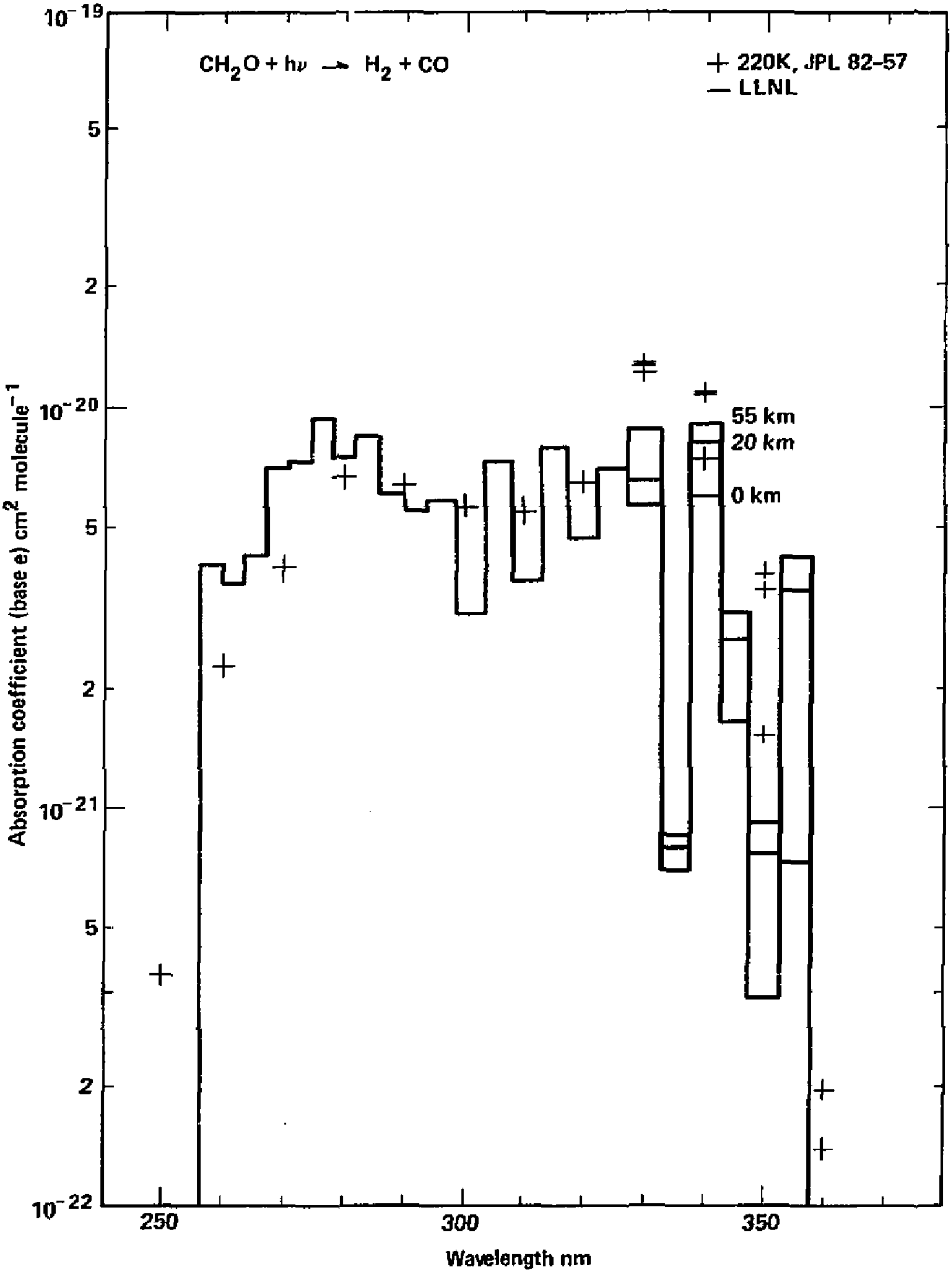

Figure 10. Effective absorption coefficients for molecular products (H_2 + CO) in CH_2O photolysis. At 330 nm and above the coefficients are calculated as a function of altitude and values corresponding to 0, 20, and 55 km are shown. Also plotted are the recommendations of DeMore et al. (1982) for these altitudes. Temperature dependence is small and is not shown.